frontiers in Earth Science

ORIGINAL RESEARCH
published: 16 December 2020
doi: 10.3389/feart.2020.548251

Post-Caldera Eruptions at Chalupas Caldera, Ecuador: Determining the Timing of Lava Dome Collapse, Hummock Emplacement and Dome Rejuvenation

Marco D. Córdova, Patricia Ann Mothes, H. Elizabeth Gaunt and Josué Salgado*

Instituto Geofísico, Escuela Politécnica Nacional, Quito, Ecuador

Determining the lithology, extent, origin, and age of hummocks can be challenging, especially if these are covered by successive deposits and lush vegetation. At Chalupas caldera, a late-Pleistocene silicic center that lies astride the Eastern Cordillera of northern Ecuador, we have tried to overcome these difficulties by combining geological observations and sampling, laboratory analysis (geochemistry, scanning electron microscope analysis and radiometric dating) and remote sensing techniques. Chalupas is the second largest caldera in the Northern Volcanic Zone of South America and its VEI 7 eruption, which occurred ~0.21 Ma, has garnered the attention of the volcanological community. Our research highlights new observations of the post-caldera activity at Chalupas, beginning with the growth of Quilindaña stratovolcano (~0.170 Ma), followed by the formation of Buenavista dome that is located 5 km eastward of Quilindaña's summit. At the eastern foot of Buenavista dome we identify hummocky terrain covering an area of ~20 km^2. Collectively, the suite of techniques that we used helped to highlight geological features that shed light on the provenance of the hummocks and demonstrate that this topography may have originated from gravitational breccia flows from Buenavista lava dome. Numerical simulations were also performed to represent breccia flow transit and emplacement over the present caldera landscape and to view the potential hazard footprints of a future Buenavista dome collapse. For modeling we employed volumes of 20–120 Mm^3 to visualize the consecutive traces of mass flow deposition and how the traces correspond to the hummocky landscape. Following the partial collapse of Buenavista lava dome, its rejuvenation is represented by tephra layers of several small eruptions that are dated at about 40 ky BP. These tephras represent some of the youngest eruptive activity recognized at Chalupas caldera. Our results contribute to the overall knowledge about Chalupas and demonstrate that eruptions at this important caldera are more recent than was previously reported.

Keywords: Buenavista, Chalupas caldera, scanning electron microscope imaging, field mapping, volcanic hazards, dome collapse breccia

OPEN ACCESS

Edited by:
Pablo Tierz,
The Lyell Center, United Kingdom

Reviewed by:
Alessandro Tibaldi,
University of Milano-Bicocca, Italy
Jon J. Major,
United States Geological Survey (USGS), United States

****Correspondence:***
Patricia Ann Mothes
pmothes@igepn.edu.ec

Specialty section:
This article was submitted to Volcanology, a section of the journal Frontiers in Earth Science

Received: *01 April 2020*
Accepted: *18 November 2020*
Published: *16 December 2020*

Citation:
Córdova MD, Mothes PA, Gaunt HE and Salgado J (2020) Post-Caldera Eruptions at Chalupas Caldera, Ecuador: Determining the Timing of Lava Dome Collapse, Hummock Emplacement and Dome Rejuvenation. Front. Earth Sci. 8:548251. doi: 10.3389/feart.2020.548251

INTRODUCTION

As stated by Paguican et al. (2012) *"Hummocks are the morphological expression of brittle layer deformation due to spreading in landslides and avalanches. They are principally the stretched remains of tilted and rotated blocks of the original failure volume."* Sometimes it is difficult to know the processes that led to lava dome or sector collapse and subsequent hummock formation, especially if the hummocks were formed tens of thousands of years ago in a rainy environment, such as at Chalupas caldera.

Since the eruption of Mount St Helens in May 1980, in which the first well-observed debris avalanche deposits were emplaced (Voight et al., 1981; Voight et al., 1983; Glicken, 1996), researchers are more attuned to identifying hummocky morphologies around volcanoes. Also, it is now commonly accepted that hummocky morphologies are often indicative of the occurrence of lava dome collapse or flank collapses (van Wyk de Vries and Davies, 2015). Volcanic lava domes are characterized by highly viscous solidified or semi-solidified masses of extruded lava at a volcano. When lava domes collapse they often generate block-and-ash flows, sometimes with little warning (Calder et al., 2015). These block-and-ash flows may form hummocky terrain, such was the case at Soufriere Hills Volcano, Montserrat (Sparks et al., 2002).

On a larger scale, the failure of an entire volcanic flank can involve substantial volumes of lithic fragments, of one to tens of cubic kilometers, with runout distances of over 80 km from source, especially if the flow is channelized, as is the case at Raupehu volcano in New Zealand (Tost et al., 2014). Similarly, the runout for a 100 km long debris avalanche from Colima volcano, Mexico, reached the Pacific ocean (Stoopes and Sheridan, 1992). At Shasta volcano, United States, the collapse of a portion of the edifice provoked a debris avalanche which covered a broad plain and the angle of dispersion of the hummocks spanned approximately 40° (Crandell et al., 1984). Clast-rich hummocks originated from a sector collapse ~4,500 years BP on the northern flank of Cotopaxi volcano, Ecuador and upon deposition these hummocks were covered by a lahar deposit (Mothes et al., 1998). The latter example demonstrates the need to conduct careful fieldwork that considers all options that may have contributed to either create or modify hummocks. Local environmental conditions, past and present, play a key role in the preservation or destruction of the original characteristics and fabric of the avalanche deposit within hummocks.

While Chalupas caldera is best known for producing a large ignimbritic deposit (Hammersley, 2003) (**Figure 1**), an area stretching eastward from the foot of Buenavista lava dome on the Chalupas caldera also draws attention. There we observe a landscape with several hundred hummocks whose sizes range from a mere 10 m diameter and 10 m high to more than 200 m diameter and ~30 m high. The largest hummocks concentrate in the center area, while on the margins their dimensions are smaller. Our hypothesis is that the hummocks may be the product of a gravitational lava dome collapse. Their forms, distribution, clast homogeneity, varied sizes and lack of convincing evidence of heat set them apart from glacier or lahar deposits, planar pyroclastic density current deposits undergoing erosion and also from discrete block-and-ash flows originating from limited dome destruction. Thus, to gain an improved perspective on the hummocky terrain and to visualize and capture the distribution of flow emplacement, we apply remote sensing techniques, scanning electron microscope (SEM) image analysis and field mapping. Computational modeling also shows the footprint upon the terrain if the actual, but now inactive Buenavista lava dome collapsed, spreading out over the present topography.

There are a number of key issues we sought to resolve in this study, and these include:

What is the extent of the area covered by the hummocks?
What are the lithologies of the hummocks?
What is the approximate age of the hummock field and the subsequent eruptive activity of Buenavista lava Dome?
What volcanic event might have led to the formation of the hummocks at Chalupas caldera?
Can computational modeling, run on the present (modified since 40 ky) topography, produce hazard footprints that are comparable to the measured area of the hummock field?
Which mass-flow volumes, as an order of magnitude, can best represent the area covered by the hummock field?

THE ECUADORIAN ANDES AND THE CHALUPAS CALDERA

The Ecuadorian Andes mountain range is part of the "Northern Volcanic Zone" (NVZ) which is formed by subduction of the northern segment of the Nazca plate beneath the South American plate with a subduction rate of ~5–6 cm/year (Guillier et al., 2001; White et al., 2003; Nocquet et al., 2014; Yepes et al., 2016). The main volcanic arc consists of two parallel mountain ranges, called the Eastern and Western Cordilleras, which are separated by a structural depression known as the Inter-Andean Valley (Hall et al., 2008). The Western Cordillera consists of about 20 andesite to dacite volcanoes built upon mid-to late-Cretaceous accreted oceanic terrain (Vallejo et al., 2019), whereas the Eastern Cordillera has some 25 volcanoes, mainly andesitic, and its base is comprised of Paleozoic to early Cretaceous age metamorphosed rocks of continental affinity (Spikings et al., 2001; Baby et al., 2013; Spikings et al., 2015). The rear-arc is defined by four volcanoes: Pan de Azucar and Yanaurco (Pleistocene) and Sumaco and the Puyo cones (Holocene) (Hall et al., 2008).

Volcanism in the Ecuadorian Andes is mainly andesitic in nature (Hall et al., 2008; Hidalgo et al., 2012), and collapsed silicic calderas are infrequent. Several collapse caldera structures, including Chalupas, are recognized, lying astride the Eastern Cordillera backbone (Mothes and Hall, 2008). Chalupas caldera lies 80 km southeast of Quito and 15 km SE of the bimodal Cotopaxi volcano (Hall and Mothes, 2008) (**Figure 1**).

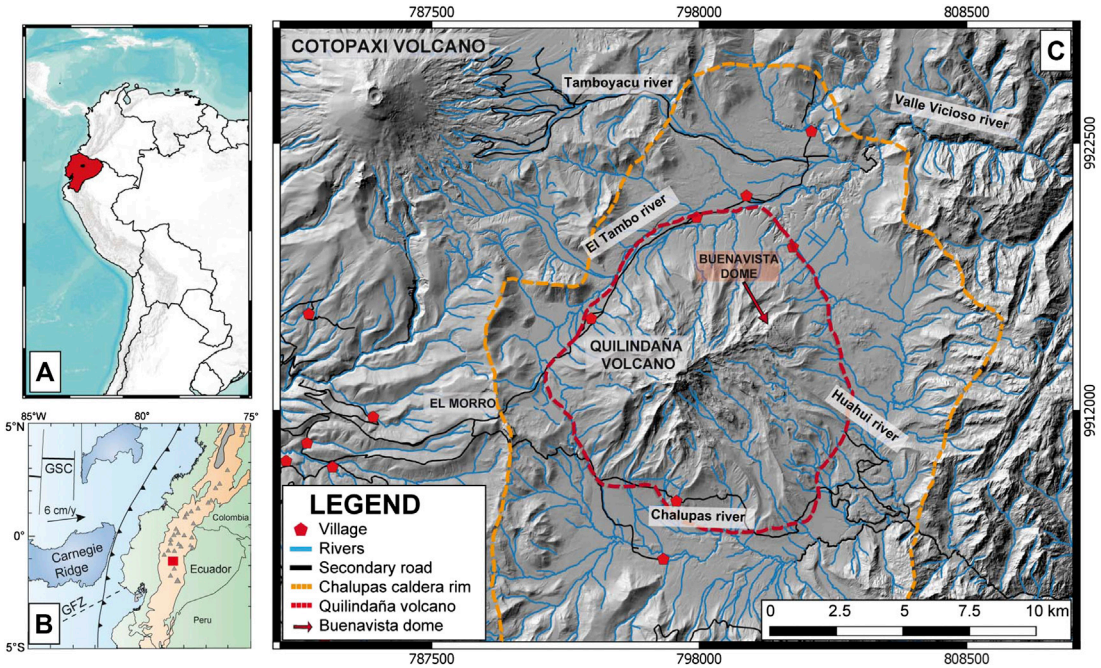

FIGURE 1 | Location of Chalupas caldera. **(A)** Ecuador. **(B)** Geodynamic framework of the Ecuadorian volcanic arc at the convergence of the Nazca and South American plates, converging eastward at 6 cm/years (White et al., 2003). The trench is represented by the black line with indents, GSC, Galápagos Spreading Center; GFZ, Grijalva Fracture Zone (modified from Robin et al., 2010). Chalupas caldera is represented by a red square. **(C)** Chalupas caldera in the local context with its topographic rim and the perimeter of Quilindaña volcano.

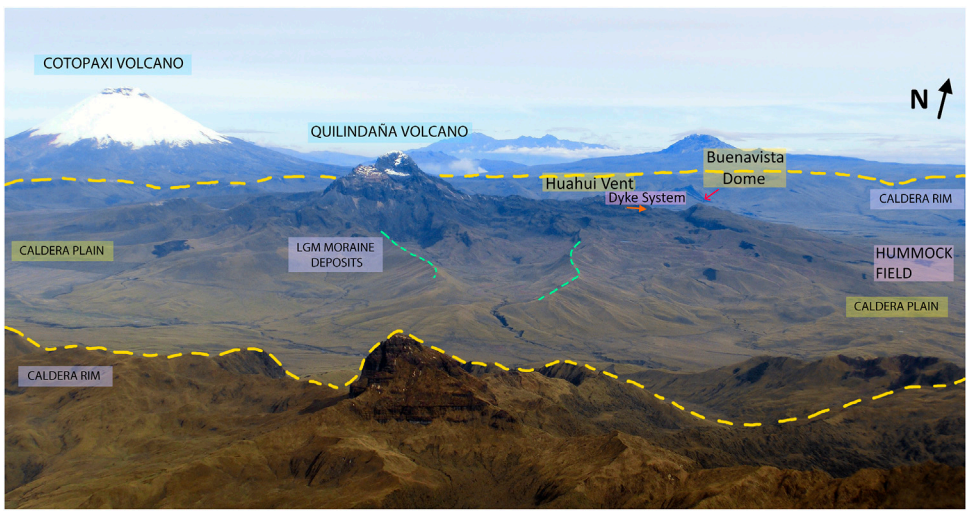

FIGURE 2 | Aerial view of the main structures of the Chalupas caldera, view toward W-NW, taken from above and slightly east of the caldera's eastern rim (yellow broken line). LGM refers to moraines of the Last Glacial Maximum period and are demarcated by green lines.

Chalupas caldera has an elongated SW-NE planform with an average diameter of ~17 km (**Figure 2**). Its formation followed one large rhyolitic eruption, causing foundering and inward collapse. Its most notable deposit is called "The Chalupas Ignimbrite" (Beate, 1989) and is dated with the $^{40}Ar/^{39}Ar$ method at 0.211 ± 0.014 Ma (Hammersley and DePaolo, 2002; Hammersley, 2003; Beate et al., 2006) and the K-Ar method at 0.216 ± 0.005 Ma (Bablon et al., 2020). The deposit has a radial distribution spreading out from the caldera rim into the Inter-andean Valley (IAV) (Beate, 1985), and related fine-grained layers are preserved on the coastal plain (Jackson et al., 2019) and in the eastern Amazon Basin.

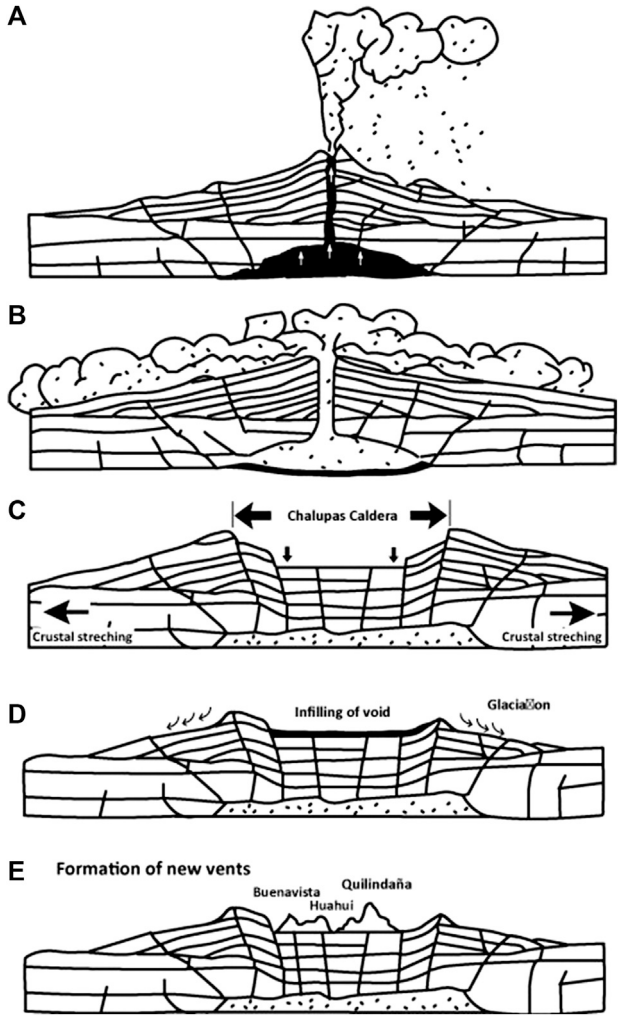

FIGURE 3 | Phases of formation of the Chalupas Caldera: **(A)** Upwelling of magma in center volcano, starting with a Plinian eruption column, with accompanying ring fracture andesitic cones forming outer boundary; **(B)** Magma evacuates the caldera and expulses ash-flow sheets to the E, W, S and N; **(C)** Collapse, foundering of caldera; **(D)** Erosion and infilling of void and glaciation; **(E)** Growth of Quilindaña peak, vent migration along dykes to the east and formation of Huahui vent and Buenavista lava dome.

Chalupas Ignimbrite

The ignimbrite deposit is a notable stratigraphic marker that contributes in determining relative ages within Ecuador's Inter-Andean Valley stratigraphy and in neotectonic studies (Fiorini and Tibaldi, 2010). The area covered by the ignimbrite is around 2,000 km^2 and the average thickness is approximately 30 m, providing an estimate of total bulk volume for the ignimbrite at around 100 km^3 (Beate, 1985; Hammersley, 2003). According to Bablon et al. (2020), the total bulk volume of both ignimbrite and associated co-ignimbrite deposits amounts to ~230 ± 30 km^3. The non-welded rhyolitic ignimbrite is crystal-poor, with scarce biotite and plagioclase crystals and typically displays large (25 cm diameter) pumice clasts with well-defined tubes. The magmas are highly evolved with SiO_2 values of 72–74 wt%.

The ignimbrite/co-ignimbrite volume ranks the eruption at a VEI 7, consistent with the associated caldera size of between 16 and 18 km diameter (INECEL, 1983; Beate, 1985; Lipman, 1997; Bablon et al., 2020). In the center of the caldera is the post-caldera andesitic volcano, Quilindaña (4,800 m), of which Buenavista lava dome (4,230 m) forms the eastern extreme (Hammersley, 2003; Córdova, 2018; Córdova et al., 2018).

Based on our fieldwork and that of Hammersley (2003), we suggest that the succession of formative events at Chalupas Caldera can be synthesized in the following stages (**Figure 3**):

Quilindaña Volcano

Shortly after the caldera collapse, a pulse of new magma began forming the andesitic stratovolcano, Quilindaña, located in the caldera's center. It has at least two main sub-phases are identified on its peak (**Figure 3E**):

(1) Quilindaña I (Initial phase), composed by amphibole andesite, which is altered due to past fumarolic activity of Quilindaña. Rocks from this phase are exposed on edges of glacial valleys (**Figure 4A**).
(2) Quilindaña II (Second phase) is composed of a pyroxene andesite which crops out at the top of the sequence and has glassier composition: an olivine-rich andesite is at the bottom of the sequence (**Figure 4B**).

$A^{40}Ar/^{39}Ar$ radiometric age, obtained on plagioclase from a sample taken from the center of Quilindaña I, is reported by Hammersley (2003). The date of 0.169 ± 0.001 Ma is interpreted as the age of the formation of Quilindaña peak and represents post-collapse activity of the caldera, following paroxysmal caldera formation about 40,000 years earlier. We recognize morphological traces of a probable sector collapse on the SE flank of Quilindaña peak. But due to glacial erosion and burial by lava flows, the collapse remains are obliterated (**Figure 5**).

Buenavista Lava Dome

Buenavista is a lava dome that formed at the northeast-east extreme of a propagating dyke system that extends 5 km east of Quilindaña peak. Between Quilindaña and Buenavista is another vent, Huahui, which emitted a 7 km long lava flow that flowed southeast to the caldera outlet carved out by the Chalupas river. Buenavista is dacitic and is more evolved than either Quilindaña or Huahui. The samples collected from Buenavista dome have compositions ranging from 61.6 to 69.5 wt% SiO_2. Petrographic descriptions and geochemical analysis show that the magma is one of the most acidic products of the post-caldera phase (Córdova, 2018).

Buenavista dome occupies about a 1.7 × 1.5 km area and has 700 m of relief above the eastern Chalupas plain. Our calculations give an approximate volume of 0.96 km^3 for the present-day Buenavista dome.

The Chalupas caldera has been affected by glacial processes both on its edges and at Quilindaña volcano (Hastenrath, 1981). We observe U-shaped valleys and sequences of both lateral and end moraines. The largest moraines, which were most active between ~36 and 13 ka (Clapperton, 1993), correspond to the

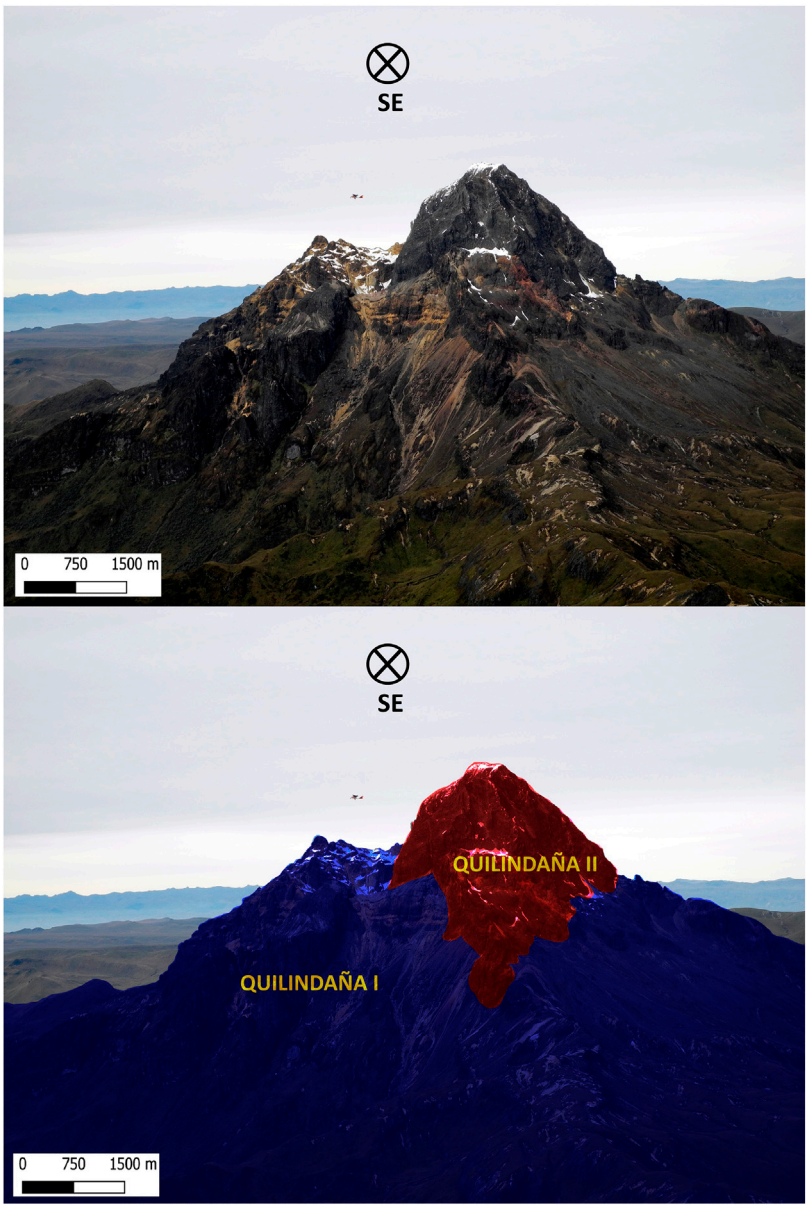

FIGURE 4 | (A) Quilindaña volcano view to the southeast. **(B)** Formation scheme of the two phases of Quilandaña. Ultralight plane is flying behind Quilindaña I.

Last Glacial Maximum (LGM) and can be found down to about 3,700 m elevation. Smaller Younger Dryas period moraines (12–10 ka) are found above 3,800 m elevation (Clapperton et al., 1997; Heine, 2004) (**Figure 2**). It is important to clarify that the hummock terrain on the eastern Chalupas plain lies below the LGM moraine limit and hummocks are not overridden by LGM moraines.

Our focus in this contribution is the study of the post-collapse phase of this potentially active caldera, aiming to account for the most recent eruptions through study of the hummocks at the base of Buenavista dome and the companion tephra layers. We elucidate the relative youthfulness of the post-caldera stage of the caldera and provide comment on potential hazards to downstream communities and projects, using our computational modeling results.

METHODS AND TECHNIQUES

Fieldwork

Our fieldwork was carried out from late 2016 to early 2020, over 7 trips of 5 days each. Access to most outcrops is by walking over high (3,600–4,400 m) alpine grasslands or riding on horseback, if swampy conditions permit. The best available stratigraphic exposures were along rivers or in road cuts. Our work concentrated on Buenavista dome and its feeder dikes,

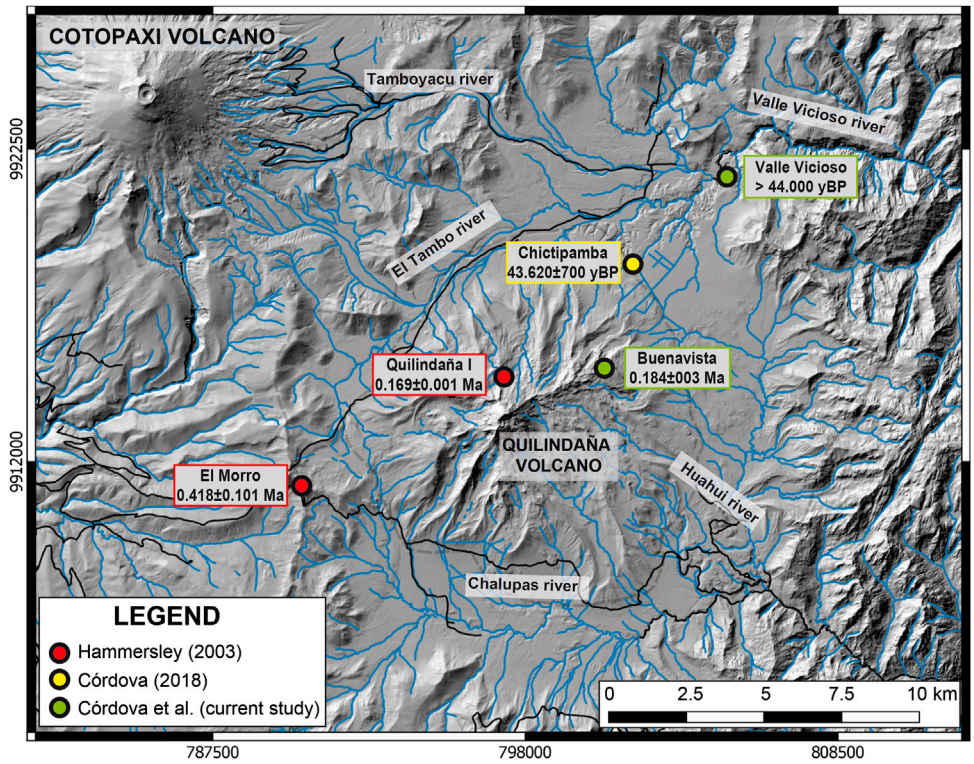

FIGURE 5 | Distribution of the radiometric ages from Hammersley (2003) (red circles), Córdova (2018) (yellow circle) and (current study) (green circle).

inspecting and mapping the hummocky terrain and identifying new ash layers that were thicker and had larger pumice and lithic sizes, compared to those emitted by other nearby volcanoes. Mineralogy is also a key factor to identify tephra origins. Based on our observations in the caldera, hornblende is present only in Buenavista dome rocks. Representative rock clasts were collected from all main lava flows and eruptive centers and analyzed for major and minor elements at the Peter Hooper GeoAnalytical Lab, Washington State University in Pullman, WA, United States. Samples of organic-rich material extracted from scarce peat layers were sent to Beta Analytic Laboratory in Miami, Florida, United States for radiometric dating (^{14}C and AMS).

Scanning Electron Microscope Image Analysis

Representative samples of rock were taken from Buenavista dome and from the interior of the hummocks and analyzed using a VEGA Tescan SEM. Samples were cut into thin wafers and polished prior to analysis. Backscatter electron images (BSE) were taken on representative areas of the samples using a 15 kV accelerating voltage, at ×100 and ×500 magnification.

Digital Elevation Map Analysis

All the geographic information was analyzed using Quantum GIS (Version 3.4) and ArcMap (Version 10.5) software. Initially, using a 3m/pix resolution DEM (Source: Instituto Geográfico Militar-Quito, 2015), which covers the entire caldera, we identified hummocky topography at the base of Buenavista Dome, spreading eastward over the caldera plain. Later we used *Topohazard*, a Linux script developed to calculate the vertical topographical differential between slopes, and which applies a color scale to smooth visual results (Marrero et al., 2019), visually enhancing the hummocky topography in the caldera.

Unmanned Aerial Vehicle Photography With a senseFly eBee Classic Drone and DEM Generation

Since the eastern Chalupas plain has difficult access due to swampy conditions, we designed a drone survey to take aerial photographs with the aim of making a higher-resolution DEM, specifically to model the emplacement of potential future breccia deposits borne off Buenavista Dome. We recognize that topography has likely undergone many modifications in 40 ka, therefore our approach is to use the present topography to model potential breccia flow emplacement. To perform the survey, we used an unmanned aerial vehicle (UAV), the eBee Classic, which is a fixed wing type drone, developed by SenseFly (**Figure 6**). To plan the survey and the flight path of the drone, we used the software eMotion 3 (designed for Windows) installed on a laptop which was used as a ground base station. The altitude of the area of interest is above 3,550 m a.s.l. with a maximum of nearly 3,800 m a.s.l. The chosen location for take-off and landing, as well as the ground station, has an elevation of 3,600 m a.s.l.

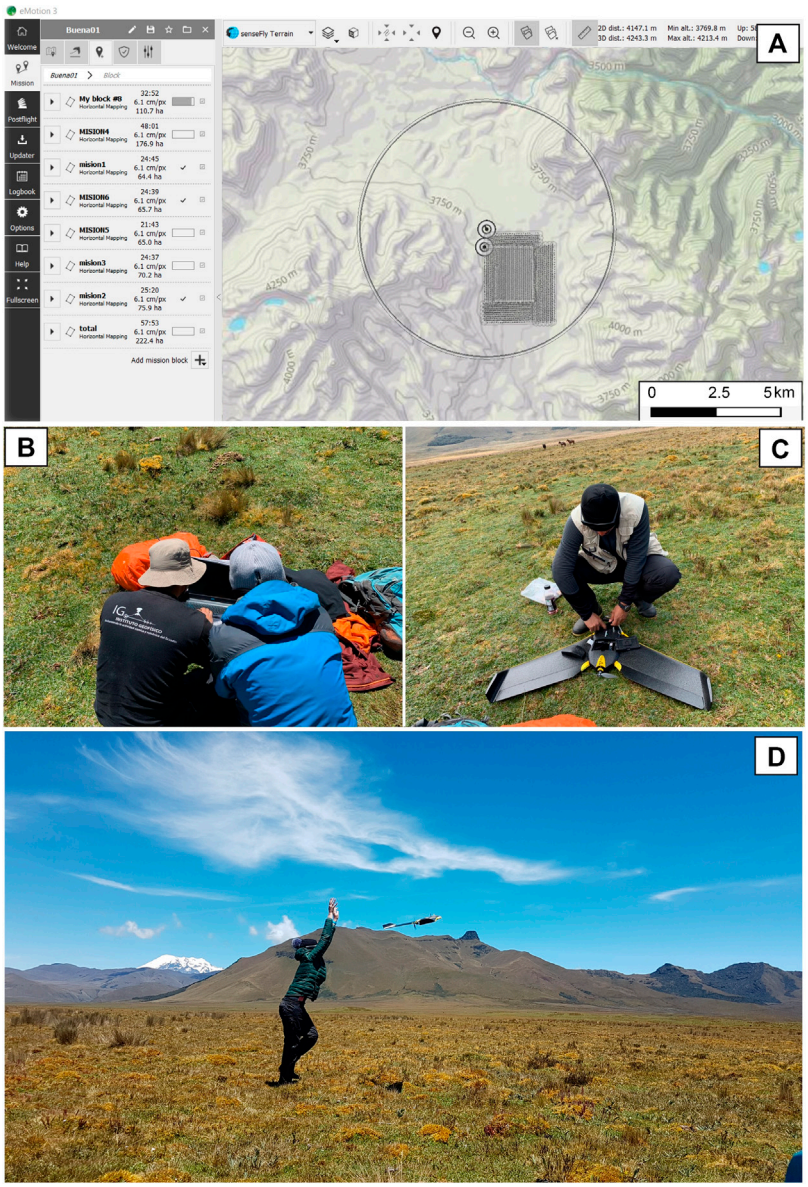

FIGURE 6 | Mosaic of the preparation for the drone survey. **(A)** Drone survey development on eMotion three software, **(B)** Ground station and flight planning on eMotion software. **(C)** Change of batteries after landing **(D)** Launching of the drone.

The survey area covered by the flights was approximately 12 km^2 and the average height of the flights was approximately 120 m above ground surface. More than 5,000 photos were taken with a Canon S110 Near-Infrared (NIR) camera with a resolution of 12 megapixels. This camera takes photos in the Near-Infrared band and red and green visual band. We used the NIR camera to avoid including clouds in the images and this type of camera also gives better results when conditions are foggy. While this may not be the main motivation to use a NIR camera, it provided images with excellent resolution to make the DEM. The dense sequence of photos recorded was processed using the software Agisoft Photoscan, version 1.5. This software works by building a dense mesh of points with a 70% lateral and longitudinal overlap on each photo in order to construct a high-resolution digital surface model and then a digital elevation model.

Geographic Data Analysis, Description of Hummocky Terrain Patterns, Volume Deposit Calculation

The result of the UAV survey over a 12 km^2 area produced a DEM with a spatial resolution of 1.5 m/pix, and produced a high quality hillshade in terms of the elevation data from the DEM (**Figures 7A–C**). The GPS of the eBee classic drone has an

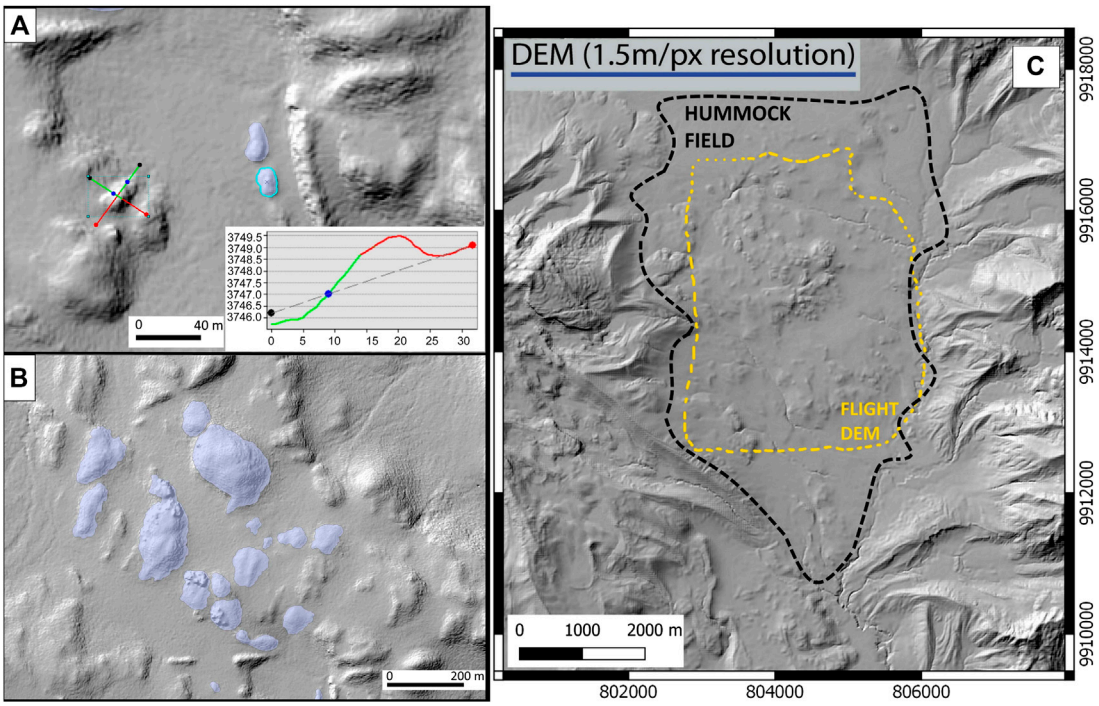

FIGURE 7 | DEM with a high spatial resolution of 1.5 m/pix which is a final result of the unmanned aerial vehicle survey. Insets **(A,B)** show polygons used to delimitate hummocks in order to derive their volume. **(C)**. The perimeter of the mapped hummock field is delimited by a broken black line, while the yellow line delimits the flight paths. BVD, Buenavista Dome.

accuracy of <3 m. Previous to our field campaign we made tests with ground control points with known coordinates, but found no significant difference between results.

Elevation profiles (**Figure 7A**) were useful to delimit each hummock with a polygon (shape files). Once we calculated the coordinates of the nodes from the borders of every polygon (**Figure 7B**), we were able to calculate the volume of the hummocks with a script written in MATLAB (Aguilar, 2013). The algorithm script calculates the volume of known polyhedrons using an interpolated grid between the coordinates of the polygons over the elevation data of a high-resolution DEM. A total of 168 representative hummocks which spread out on the east Chalupas plain were delimited, taking into consideration the relief of the hummock above its base. In earlier studies this method was used for calculating the volume of lava domes at Pululahua Volcanic Complex (Vásconez et al., 2015), hummock deposit volumes of Cotopaxi's debris avalanche (Encalada and Bernard, 2018) and the volume of eruptive vents on Wolf and Alcedo volcanoes in the Galapagos islands (Pérez, 2020).

Numerical Simulations

We ran numerical simulations of gravitational flows to compare the results to the mapped hummocky terrain draping the present landscape. We assume that the landforms of 40 ka were somewhat different than those of today due to modifications of the drainage networks. As commented upon by Özdemir et al. (2016), uncertainties in topography are a problem when trying to model older gravitational flows. Our modeling exercise helped to visualize where a future dome collapse breccia might reach onto the east Chalupas plain.

We used two numerical models: a modified version of LaharZ_py (Schilling, 2014), called *LaharZ/PFz* (Widiwijayanti et al., 2009) and VolcFlow (Kelfoun and Druitt, 2005). VolcFlow is a code which runs in MATLAB and is principally based on the depth-averaged approximation. It applies a topography-linked coordinate system, with x and y parallel to the local ground surface, h as vertical and with a depth-averaged set of equations of mass and momentum conservation. On the other hand, LaharZ_py (Schilling, 2014) is written in Python and is a tool used in conjunction with ArcMap, a Geographic Information System (GIS). Primarily, LaharZ_py is a computational model that employs statistical descriptions of areas inundated by past mass-flow events to forecast areas likely to be inundated by hypothetical future events (Iverson et al., 1998; Schilling, 2014).

We sought to simulate the flow and deposition of gravitational "dry" breccia flows. Therefore the modified version of LaharZ_py called *LaharZ/PFz,* described by Widiwijayanti et al. (2009) and developed to simulate block and ash-type PDCs, seemed the most suitable. In this case the area and cross sectional equations were modified in accordance with the semi-empirical equations A= (0.05 modified to 0.1) $V^{2/3}$, B= (35 modified to 40) $V^{2/3}$, as described by Widiwijayanti et al. (2009). The results give an objective means to assess cross sectional (A) and planimetric (B) areas to be inundated by block-and-ash pyroclastic flows of

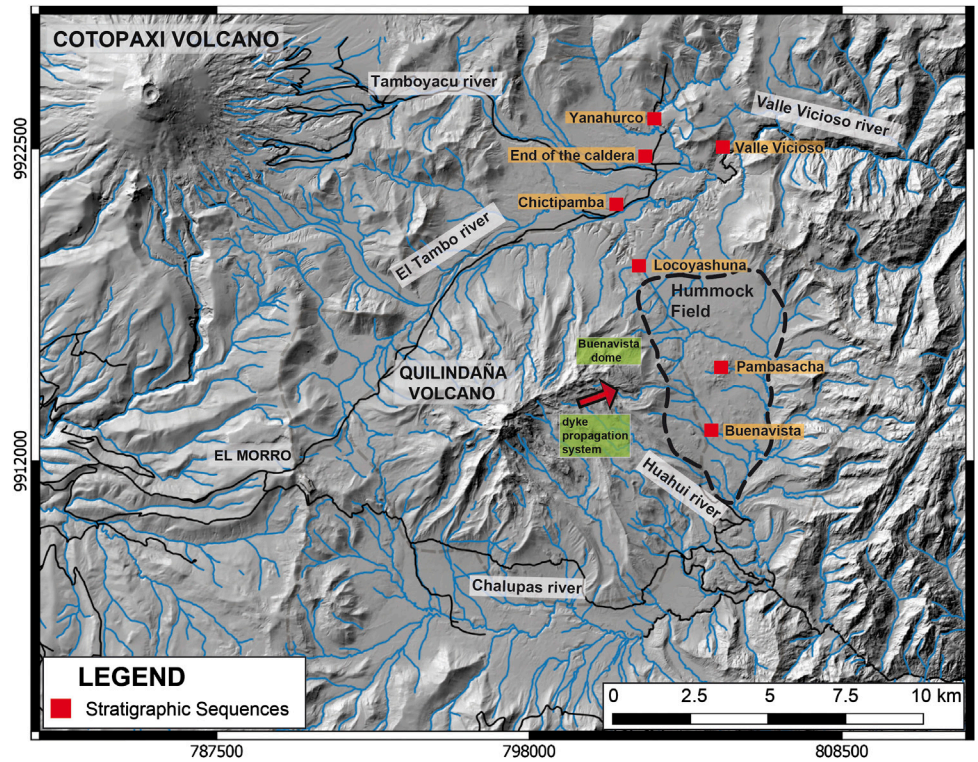

FIGURE 8 | Map showing hummock topography related to the Buenavista Dome fan on the eastern Chalupas plain, in the vicinity of Pambasacha and Buenavista stream cut sequences, and location of stratigraphic sequences discussed in the text. Mapped hummock field perimeter is delimited by broken black line and occupies the eastern Chalupas plain, which is confined between the Buenavista dome massif and steep - relief topography to the east.

various volumes (V). The program *LaharZ/PFz* does not provide information on deposit thickness. Hayashi and Self (1992) showed in a comparative study between parameters of deposits of 40 volcanic debris avalanches and pyroclastic flows that there is no discernible difference in H/L vs volume. Furthermore, they adduced that the emplacement mechanisms of the two flow types are probably very similar.

Before running VolcFlow, several inputs are required: the source location, time interval of the run, the eruptive and depositional phase of the phenomena, and other values that correspond to the particular rheological behavior of pyroclastic or avalanche flows. We applied the calibrated parameters used in VolcFlow flow modeling of two Ecuadorian volcanoes, Tungurahua (Kelfoun et al., 2009 and Sangay (Ordóñez et al., 2011). These parameters included designating values for the constant retarding stress (i.e. yield strength) variable. For example, a constant retarding stress of 50 kPa during flow was assigned for the emplacement of the Socompa debris avalanche (Chile), enabling a long runout and ample spreading of the avalanche (Kelfoun and Druitt, 2005) in the modeled results in order to match the actual trace of the deposit in the field. For the pyroclastic flows of Tungurahua's August 16, 2006 eruption, a constant retarding stress of 5 kPa was assigned for modeling the flows' emplacement, and gave very good results with regards to the mapped volcanic deposit (Kelfoun et al., 2009). For modeling Sangay's pyroclastic flows a constant retarding stress value of 4.5 kPa was employed in the VolcFlow modeling. Kelfoun et al. (2009) noted that flows with thick fronts must be modeled with a higher constant retarding stress value and at Socompa, the higher value (50 kPa) applied for this variable, represents adequately the thicker flow deposits of Socompa's avalanche deposit (Kelfoun and Druitt, 2005). For the two scenarios of our VolcFlow modeling we opted to employ the variables assigned to Tungurahua and Sangay, since our team had experience in these case studies and the similarity of rock chemistry. We acknowledge however that the yield strength values chosen may be too low, since the modeled Buenavista breccia flow did not spread out widely nor travel far enough compared to the mapped hummock trace.

Alternatively, running *LaharZ/PFz* only requires two initial parameters: a starting point and an estimated volume to begin simulating the flow phenomena. In our case, the starting point to simulate the dome collapse was the top of Buenavista dome (4,230 m.a.s.l), where the dyke propagation system which traverses from Quilindaña volcano may represent the source for new magma injection that led to dome growth. We also choose initiation at this high point because the unusually steep morphology on the eastern scarp of Buenavista lava dome suggests that there could have once been an appendage of the dome located immediately east of it (see **Figure 8**).

RESULTS

Tephra Layers From Buenavista Dome Complex

Study of stratigraphic sections in the river valleys near the base of Quilindaña volcano inform us about past activity of the local vents inside and around the caldera. Most stratigraphic sections are dominated by Holocene and earlier tephra fall deposits from rhyolitic eruptions of nearby volcanoes, Cotopaxi and Chaupiloma. Two lithic/tephra layers, here named A and B, which have angular dacitic clasts, scarce pumice and display a different mineral assemblage than that displayed at either of the two mentioned volcanoes, are deemed to be related to Buenavista dome complex. Also, a newly identified crystal-poor rhyolitic (73 wt% SiO_2) pumice lapilli layer provides possible evidence of an eruption of a silica-rich cap on top of a "crystalline mush" in the magmatic storage area (e.g., Bachmann and Bergantz, 2008). We derived a ^{14}C age of 43,620 ± 700 yBP from a peat layer beneath this siliceous ash layer. The source of this ash is also likely related to Buenavista dome and was discriminated from Cotopaxi and Chaupiloma volcanoes, based on different geochemistry and petrography (Hall and Mothes, 2008; Garrison et al., 2011; Córdova, 2018).

Stratigraphic Relationships of Tephra Layers, Breccia and Geochronology

Around the NE edge of Buenavista dome is an inclined fan with limited vertical exposure, except in stream cuts. The hummock field, shown in **Figure 8** with respect to the Buenavista and Pambasacha streams, represents higher topography initiating at the base of Buenavista dome.

Sections that we logged are generally comprised of sequences of Holocene tephras and soils, minor glacial outwash of Last Glacial Maximum age (~36,000 to 13,000 years BP) (Clapperton et al., 1997), peat layers, stream cobble bars, reworked and primary tephra layers, co-ignimbritic fine-grained ash layers that fell into a lacustrine environment, and limited debris flows. Here we will build the case for the stratigraphy associated with Buenavista dome activity, starting with evidence of breccia layers, which may be related to a collapse event or block-and-ash flows, and ascending the sequence through the younger post-collapse explosive activity represented by tephra layers.

At the bases of cuts in the Pambasacha and Buenavista stream valleys, where breccia exposures are 5–10 m below the east Chalupas plain surface (**Figure 8**) we observe units with angular to sub-angular porphyritic dacitic clasts containing large plagioclase and hornblende crystals in a glassy to ashy matrix. Some blocks are irregular size, with a diameter up to 5 m, homogeneous, monolithologic, with jigsaw-cracks. For the matrix, grain size ranges from fine to coarse gravel to medium sand size. Occasional white pumice clasts are observed but are rare. Mostly clasts are without a vesiculated rind. The sorting is generally poor, the deposit is unconsolidated and the matrix colors are off-grey to rosy pink (**Figure 9**) of the fresher outcrops, particularly for exposures in the Buenavista stream valley section (see photos, **Figures 9A**, **A2**). These clasts are akin to those rocks comprising Buenavista dome. Iron-staining of the finer-grained, matrix facies is common (**Figure 9**, photo E). A sequence of fine-grained co-ignimbritic ash and lithic fragments in an ash-rich matrix that has a massive appearance with no layering overlies the breccia layer.

We estimate that the breccia deposit is approximately 20+ m thick based on observations of the tallest hummocks that rear out of the slightly inclined surface. Hummocks are also observed several kilometers farther to the east on the plain's perimeter which is in contact with high-relief non-volcanic ridges, and southward to the incoming Hauhui stream valley (**Figure 8**).

In the Chictipamba section, along the Tambo river's right margin, (**Figure 9**, Photo B), starting at the top of the section, we first observe Holocene tephras and soil, then Last Glacial Maximum till and peat, down to layer CHL-MC-29, which is a white pumice lapilli with biotite and hornblende crystals and which has similar but more evolved chemistry of its pumice (73 wt% SiO_2) compared to Buenavista dome samples. An underlying peat almost immediately beneath the tephra layer (sample CHL-MC-29) provides a ^{14}C date of 43,620 ± 710 years BP. While there are few lithics in the ash-rich layer, its componentry and grain size suggest that it is from a local source. The underlying 5 m thick co-ignimbritic layers of fine silt-size ash display abundant biotite crystals with lathe-forms. A lack of hornblende crystals and the presence of obsidian shards suggest a distal source up-valley from Cotopaxi, however, interbedded are fine-grained lithic layers of fallout whose source is likely Buenavista dome explosions/collapse.

Both A and B tephra fallout layers cropping out 2 km S-SE at the higher elevation Locoyashuna cut (**Figures 8**, **9**, Photo C) have abundant lithic components of gray and rosy-colored dome-like rocks and scarce hornblende-bearing pumice. The angularity of the components, their similar petrography to Buenavista dome rocks and their dimensions (1–3 cm diameter) suggest that a local vent eruption is the probable source. The lower older Tephra A contains more altered clasts and overall has a more weathered appearance than the overlying Tephra B. Comparatively, the younger upper B layer is fresher and with more angular clasts, has scarce altered clasts and biotite crystals are coppery-colored. Both tephra layers are immersed in a massive deposit with faint centimeter thick laminations comprised of angular, tabular lithics in a coarse-sand-ashy matrix.

Lastly, two fallout layers, identical to the described Tephras A and B at Locoyashuna, are observed in the intermediate portion of a 100 m deep cut on the right margin of the Valle Vicioso River, on the far eastern limit of the Chalupas Caldera (**Figures 8**, **9**, Photos D and D2). In both fallout layers, fresh, angular hornblende-bearing lithics are prominent with scarce pumice content. An AMS date derived from analyzing an underlying peat layer, near the base of the Vicioso section, provides an indeterminate age of >44,000 yBP, which is older than the age of the peat (43,620 ± 700 yBP) beneath the Chictipamba tephra layer.

Our study provides a new $^{40}Ar/^{39}Ar$ date of 0.184 ± 0.003 Ma (sample CHL-MC-15). Dating was performed by Dr Brian Jicha of the Rare Gas Geochronology Lab, University of Wisconsin-

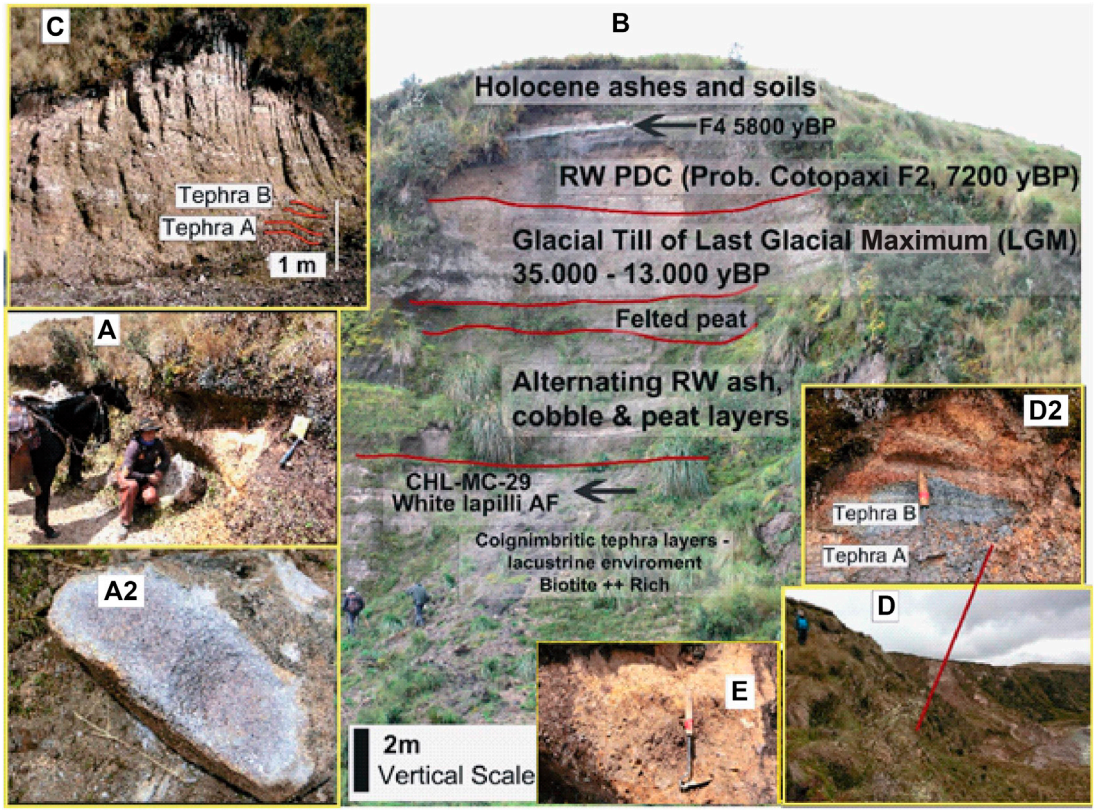

FIGURE 9 | Outcrops which display stratigraphic layers related to Buenavista dome complex. Photo **A** is of a cut in Buenavista stream valley, while **A2** is a close up of dacitic porphyritic, hornblende-bearing clast; (B) is section at Chictipamba, displaying the stratigraphic sequence, the tephra lapilli fallout layer CHL-MC-29, with a underlying date of 43,620 ± 710 years BP, and 5 m of underlying lacustrine/fine-grained layers; **(C)** is outcrop at Locoyashuna river valley where two fallout layers, **(A,B)**, predominantly of dacitic lithics, are hypothesized to be related to post dome collapse explosive activity of Buenavista dome complex; **(D)** is photo of 100 m deep cut on right margin of the Valle Vicioso River. At its base is a dated peat layer of >44 ky BP and at intermediate level are the two dacitic lithic fallout layers, **(A,B)** (photo **D2**), identical to the two layers logged at Locoyashuna cut (photo **C**). Photo E is of an iron-stained matrix facies of breccia deposit outcropping at the Buenavista stream cut. Here lithic matrix is >50%. An ashy co-ignimbritic layer caps the sequence.

Madison, on groundmass of a sample taken from the Buenavista dome summit (**Figure 5**). This age is contemporaneous with the first phase of Quilindaña I (0.169 ± 0.001 Ma), suggesting that both structures evolved more or less simultaneously in the early post-caldera phase and that the dyke feeder system has been active from the start.

Collapse of Buenavista's Eastern Flank?

Using the new 1.5 m/pix resolution DEM made from the drone flights and field observations, we identify a scar on the east limb of Buenavista dome where a possible appendage of Buenavista complex once extended and subsequently collapsed, thus forming the hummock field (**Figures 10**, **11**).

The scar left by the slide off the dome likely suffered subsequent glaciation and its morphology is now characterized by uneven terrain with numerous rock benches/ledges. LGM (Clapperton et al., 1997) moraines wrap around the Buenavista massif and descend to the base of the dome complex. Since we believe that the scar's morphology has been altered by erosional processes we did not compare our simulation volumes with an estimated volume of the scar. Additionally, in observations made by Voight et al. (2002) on the 1997 sector collapse and debris avalanche at Soufriere Hills volcano, Monserrat, the breccia deposit's volume was much greater than the volume estimated for the remnant scar due to volumetric bulking of the avalanche flow while in transit.

Moraines near to Buenavista dome are considerably shortened in their penetration onto the Chalupas plain, unlike at other sectors of the Quilindaña massif where robust LGM moraines extend down to 3,700 m elevation. This difference may reflect that the lava dome collapse destroyed or buried pre-existing moraines and that later glaciers around the Buenavista dome could not regrow and finally produce far-extending moraines. LGM moraines are present around Buenavista dome at 3700^{+} meters elevation, but are never seen over-capping hummocks.

During our field campaigns, our search on horseback along the Pambasacha and Buenavista streams (**Figures 8**, **10**), both of which originate on Buenavista dome, revealed outcrops of two different rocks types of possible dome origin. These rocks crop out some 5–8 m below the surface in a coarse sandy matrix. The

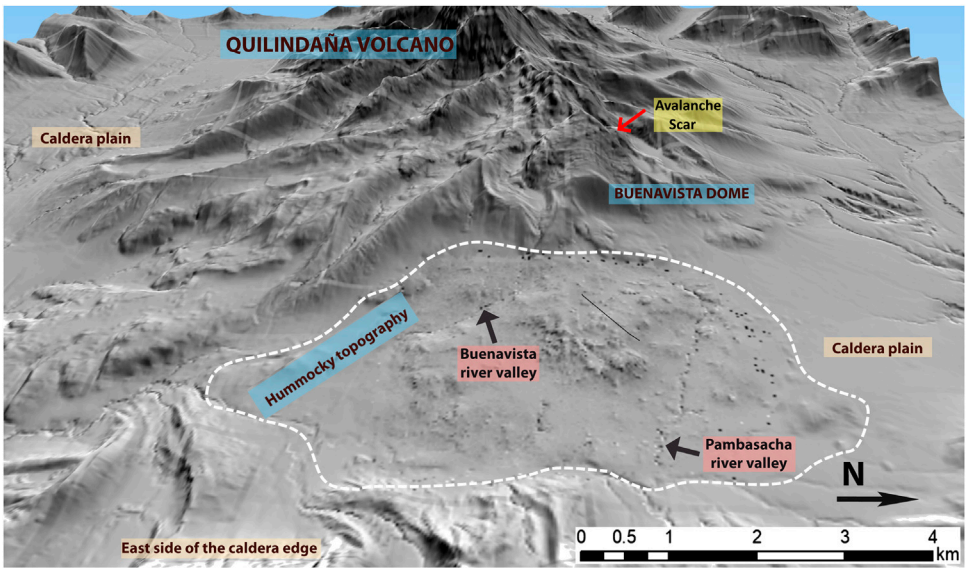

FIGURE 10 | 3D model of Buenavista dome, where hummocky topography spreads out from the eastern foot of Buenavista Dome. Top of scar indicated by red arrow. View to west.

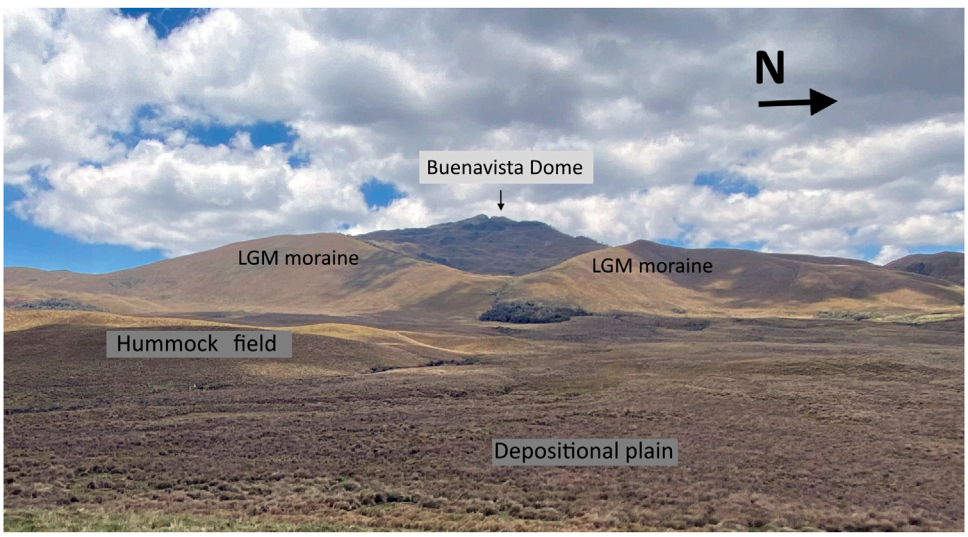

FIGURE 11 | Scar left by destruction of a portion of Buenavista dome's east flank whose resulting gravitational flow is hypothesized to have formed the hummock field, partially seen in the foreground. View west.

first category is a rose-grey colored, fresh, plagioclase-rich, semi-vesicular dacitic dome rock with crystals between 2–4 mm in size. This rock type represents the bulk of the deposit within the coarse sandy matrix which is of similar mineralogy. The second category is a dense, aphanitic black rock with large >2 mm sized plagioclase phenocrysts which are heavily altered and weathered. The first dacitic sample is most akin to present day Buenavista dome while the second sample does not have a recognizable modern cohort.

The upper Chalupas plain surface is not undergoing rapid incision by streams, attested to by swampy conditions, suggesting that the breccia may form an impermeable layer. The hummock field covers an area of about 20 km^2 and the farthest hummock cluster is located 7 km SE from the base of the dome. As mentioned, the east Chalupas plain is confined on the east by steep high-relief metamorphic ridges down to the intersection with the Huahui stream valley (**Figure 10**).

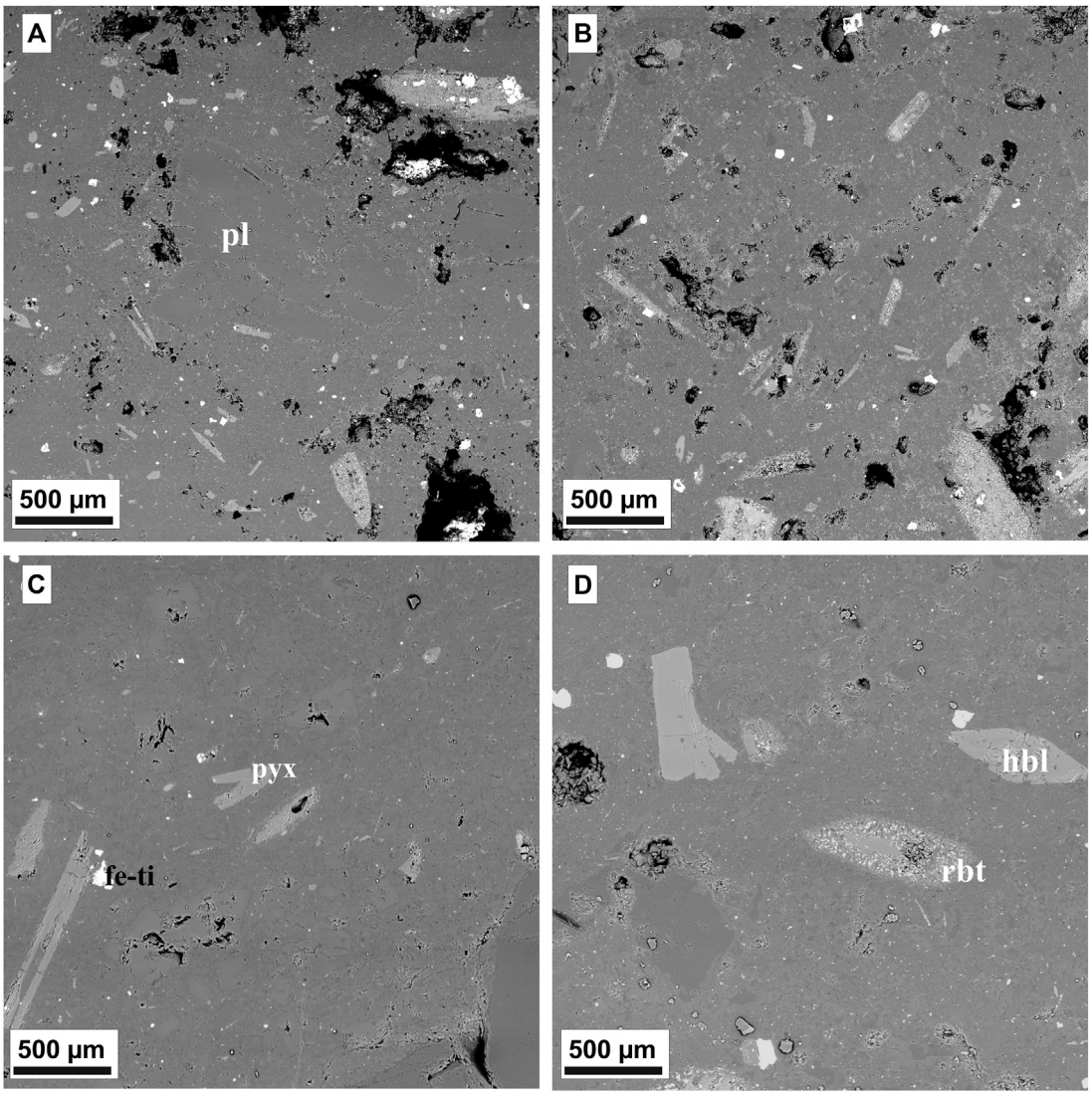

FIGURE 12 | A and **C** are of sample CHL-MC-15 (Buenavista Dome rocks) and **(B, D)** are of sample CHL-PIS-25 (Buenavista stream valley samples). Plagioclase (pL), hornblende (hbl), pyroxene (pyx) and Iron-Titanium oxides (Fe-Ti) are labeled in the images. **A** rim breakdown texture is also labeled in **D** (rbt).

Linking *In-Situ* Buenavista Dome Rocks to Breccia Samples From Pambasacha and Buenavista Stream Hummock Cuts

Samples of the Buenavista dome were collected during a field campaign in December 2016 when the remnant scar on the east flank was observed. More recently, during investigations in the Buenavista and Pambasacha stream valleys, samples of breccia were collected from outcrops in hummocks for comparison with the *in-situ* dome samples. This was done with the aim of confirming whether origin of the breccia deposit was derived from the Buenavista dome complex.

Samples taken from the Buenavista dome summit are massive, porphyritic dacite, light gray in color but often with a rosy hue. In thin section, they are hypocrystalline with phenocrysts of plagioclase (often with clay alteration products), clinopyroxene, amphibole, and metal-oxides. The matrix is microcrystalline and composed of plagioclase, orthopyroxene, and metal-oxides. SEM backscatter images were taken (**Figure 12**) of both the dome samples and samples collected from deposits in the hummocks. Samples from the breccia deposit show a marked resemblance to the samples from the dome both in appearance, composition and microstructure. As described in the stratigraphic section (**Figures 9A, A2**) the samples taken from a cut in Buenavista stream exposing the breccia deposits are light gray with a rosy hue and are porphyritic, with obvious plagioclase and hornblende crystals. The hand specimens of the two samples appear remarkably similar. Under the SEM, the similarities are even more obvious with both samples displaying large plagioclase, amphibole, pyroxene

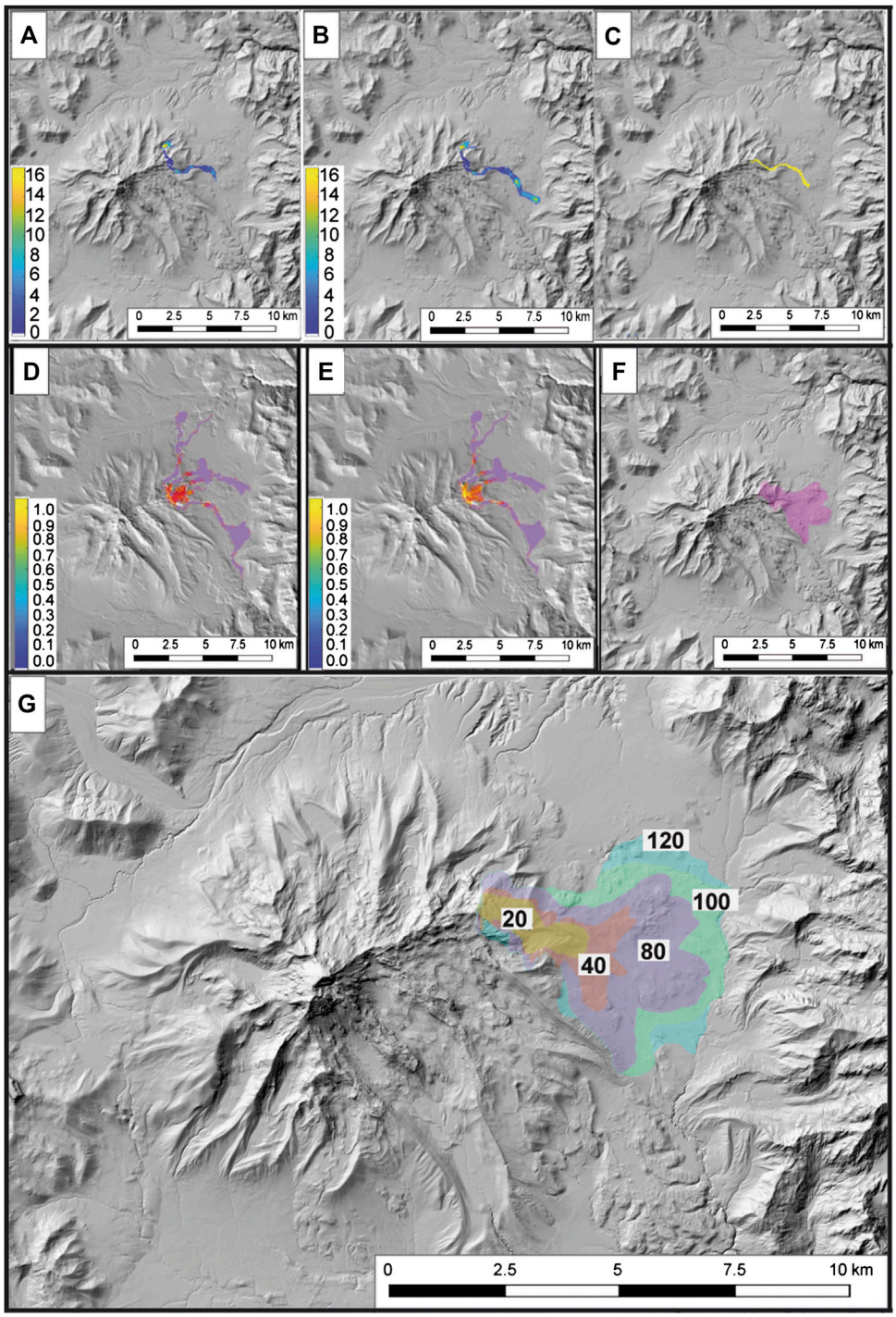

FIGURE 13 | Upper Panel **(A–C)**: Numerical results from modeling 10 million cubic meters for emplacement of a gravitational flow breccia. **(A)** Scenario I in VolcFlow, **(B)** Scenario II in VolcFlow; color bar represents thickness of deposit in meters. **(C)** *LaharZ/PFz* results (*LaharZ/PFz* does not provide thickness quantitative results). Middle Panel **(D–F)**: Numerical results from modeling a volume of 80 million cubic meters for emplacement of a breccia. **(D)** Scenario I in VolcFlow, **(E)** Scenario II in VolcFlow; **(F)** *LaharZ/PFz* results (*LaharZ/PFz* does not provide thickness quantitative results). Bottom Panel: **(G)** Nested inundation areas for 20–120 Mm^3 volumes, respectively, for emplacement of the breccia, modeled with *LaharZ/PFz*.

and metal oxide phenocrysts in a very fine ground mass composed of plagioclase, pyroxene and oxide mineral microlites (**Figure 12**). The phenocrysts present in both samples are of very similar size, shape and composition. Many of the pyroxene and amphibole phenocrysts, in both samples, also show signs of alteration and breakdown. Some of the phenocrysts

display alteration and breakdown of only the crystal rims (**Figure 12D**), while others display psuedomorph textures which result from a complete breakdown of the phenocryst (e.g., De Angelis et al., 2015). In the images of higher magnification (×500), the ground mass crystals are also extremely similar between the two samples and are dominated by plagioclase microlites with a very small quantity of glass in between.

Numerical Simulation Settings and Results

The main input data for the numerical simulations was the 3 m/pix resolution DEM. The output data of *LaharZ/PFz* is the representation of the flow footprint as a raster file. On the other hand, simulations with VolcFlow provide output data such as possible volume and velocity, based on rheological inputs. The outputs from each of the flow simulations are plotted as virtual phenomena on the initial DEM (3 m/pix special resolution) which was used since it covers the entire area of the caldera, while the higher resolution 1.5 m/pix DEM covers only the majority of the hummock field on the eastern Chalupas plain (**Figure 7C**). Neither software used for the numerical simulations can use "patched" or merged DEMs with different resolutions.

Employing the new high-resolution 1.5 m/pix DEM, we first calculated the volume of the deposit of the hummocky terrain from the polygon hummock shapes (**Figures 7A,B**), the results of which provided a total volume estimate of approximately 7 million cubic meters for the 168 identified hummocks. A limiting factor of this exercise is that only the relief of each hummock rising above the East Chalupas plain was tallied to provide the vertical component value. Therefore, this calculation gives a minimal volume of the deposit volume since it cannot estimate the buried subsurface volume, nor the volume that has been eroded. The hummock field was probably affected by post-emplacement erosion and stream reworking, which removed considerable portions of material, leaving the outstanding hummocks as testimony. In order to have a starting input volume for the modeling we increased the minimum volume of the hummocks to ~10 million cubic meters which was the volume that we applied to run the initial simulations of both *LaharZ/PFz* and VolcFlow programs (**Figure 13**). Still, this first-approximation volume is grossly under-calculated since it is not taking in consideration the volume of the deposit infilling between individual hummocks. We did not estimate this volume, given the long time that has elapsed since the collapse event, the modifications to topography and the mantling by soils and grasslands, which make detailed measurements of individual hummock profiles difficult. Hypothetically, if an average thickness of 20 m for the avalanche breccia deposit is assigned to cover the entire 20 km^2 hummock area, the total calculated volume would be on the order of 4×10^8 m^3. This is a value which we cannot vouch for, but which would also have suffered erosion and is about 40% of the actual Buenavista dome volume. Furthermore, it is unlikely that all areas of the east Chalupas plain had the same depositional thickness.

Initially, we ran the program *LaharZ/PFz* as this requires only two inputs (volume and starting point). This was a test to get initial results that would be plugged into the first simulations in VolcFlow. We summarize the two scenarios for running VolcFlow as follows with: T. represents time, T. Source is the time assigned for evacuation of mass flows from the source vent and T. Max is the duration of the flow moving over the terrain. The Cohesivity variable is the constant retarding stress (yield strength) that approximates rheological aspects of an avalanche and is also indicative of the spreading over the landscape of rock avalanches for a range of volumes (Kelfoun and Druitt, 2005).

Scenario I VolcFlow

Input parameters		References
Cohesivity	4.5 kPa	Sangay volcano, hazard map.
T. Source	3,000 s	Ordóñez et al. (2011)
T. Max	3,500 s	

Scenario II_VolcFlow

Input parameters		References
Cohesivity	5 kPa	Tungurahua volcano 2006 eruption.
T. Source	3,500 s	Kelfoun et al. (2009)
T. Max	3,500 s	

The results of running VolcFlow, applying both Scenario I and Scenario II, using different volumes, are shown in **Figures 13A,B,D,E**. The runs of *LaharZ/PFz* is shown in **Figures 13C,F,G**.

All flows reach the hummock plain, although each scenario gives slightly different, but similar results (**Figures 13A,B**). The higher cohesive value related to initial VolcFlow modeling of 10×10^6 m^3 (Scenario 1) gives a more limited reach compared to Scenario II and thickness values are on the order of 4–10 m. All flow paths, including those produced by *LaharZ/PFz*, are restricted in their lateral extent compared to the presently-observed Buenavista hummock field.

For VolcFlow results of modeling 8×10^7 m^3 we see that the flows' reach shown in **Figure 13** "d" and "e" is somewhat similar, with both scenarios taking a longer and wider path into three distinct drainages and showing very thin deposit thickness of 0.1–0.2 m. Given the considerable unknowns of the true dimensions of the hummock deposit when it was emplaced as well as the topography, we believe it is more honest and worthwhile to view our simulation exercises as forward modeling in order to understand where future flows may be directed.

Subsequently, we repeated the simulation with only *LaharZ/PFz*, incrementally increasing volumes within the range of 20–120 million cubic meters, in order to gain understanding of the extent of the inundation of future flows, should they occur at the now inactive dome (**Figure 13G**).

The results of the simulations with *LaharZ/PFz,* using 120 million cubic meters volume on the present-day landscape, take the flow out to the limit of the eastern Chalupas plain, nudging against the slopes of adjacent steep ridges and extending 7 km to the south. The modeling trace shows a reasonable association

with the perimeter of the mapped hummock field on the eastern Chalupas plain that we see today extending from Buenavista's base. It also well coincides with the densest remnant hummocky area. In sum, the mapped areas of highest concentration of hummocks are best represented by *LaharZ/PFz* simulations since they cover the full extent of the hummocky area, therefore we believe that the areal extent of the 20 km^2 hummocky zone is mostly invariable since deposition.

Hence in accordance with our fieldwork, the Buenavista hummock field as seen today is a good representative of the areal extent of the original deposit. However, the deposit thickness doubtless has experienced important variations and whatever volume is chosen will be a rough estimate. Therefore, modeling volumes based on reproducing the present extent of the deposits should be interpreted as an approximate, order-of-magnitude estimate. Our use of the 120 million m^3 volume in the modeling is defendable in general terms, as the results mantle the hummock field to its perimeter. Our results are also representative of a hypothetical new collapse of Buenavista's eastern flank using the actual topography provided by the high-resolution DEM.

Doubt is often expressed concerning remnant traces of avalanche deposits and how representative they are of when the event occurred. For the Socompa debris avalanche, researchers compared the pristinely preserved deposit (7 ka) outline of the avalanche with the modeled results (Kelfoun and Druitt, 2005); the results between the deposits on the ground and modeled results are very similar. Therefore, applying some precautions, both ground truth and modeling results can offer constraints on one another.

DISCUSSION

The VEI 7 Plinian eruption at 0.216 Ma that formed the Chalupas Ignimbrite evacuated between 100–230 km^3 of bulk volume of rhyolitic magma and provoked the collapse that formed the caldera. Then, reinjection of a more mafic magma into the magmatic reservoir formed Quilindaña stratovolcano, whose composition is andesitic to dacitic. Dyke propagation eastward of Quilindaña formed the Huahui and Buenavista vents. We identify a scar on the eastern side of Buenavista dome and observe topography on the caldera floor reminiscent of hummocky morphology generated by gravitational collapse (e.g., Crandell et al., 1984; Ui et al., 2000; Sparks et al., 2002). We suggest that the breccia deposit that comprises the hummocks is an avalanche deposit originated from a gravitational collapse on the eastern flank of Buenavista dome, resulting in a topographically well-confined 20 km^2 area covered with hummocks. This hummock field has undergone stream erosion and burial by younger ashfall layers and formation of young volcanic soils, but it has not been glaciated. The original area of hummock deposition was about 20 km^2, since broader spreading to the east was impeded by higher pre-existing topography.

From the new 1.5 m/pix DEM, created from our drone survey imagery, we determine that the hummock field has a variety of sizes and shapes. The heights of the hummocks, the steep sides on some of them, the presence of occasional large (>5 m) diameter lithic clasts that were eroded from hummock interiors and the overall lithic, non-vesicular nature of the matrix and clasts, suggest that a collapsing lava dome would be a more likely source rather than a PDC being erupted, where a more planar morphology usually results (Fruendt et al., 2000). The well-studied debris avalanche deposit laid down in December 1997 at Soufriere Volcano, Montserrat gives testimony to the chaotic nature of the interior of hummocks and the presence of megablocks which were deposited in several flow pulses during the avalanche breccia emplacement process at that volcano (Voight et al., 2002).

Through comparison of rock samples taken from Buenavista dome summit and of samples extracted from the breccia deposit within the hummock field we have shown that the origin of the deposit that forms the hummocks is most likely the Buenavista lava dome complex. The two sets of samples have the same petrological and textural characteristics (**Figure 12**). Specifically, analysis of SEM backscatter images of the collected samples show a striking similarity between the Buenavista lava dome samples and the hummock breccia deposit samples. Prevalence of similar breakdown features on amphibole and pyroxene crystals in both samples and other similarities provide significant evidence for the samples of the breccia deposit extracted from hummocks being the same as the Buenavista dome samples. These similarities therefore strongly suggest that the likely origin of the deposit that forms the hummocks was the collapse/slide of the eastern portion of Buenavista lava dome complex.

The partial collapse of the east flank of Buenavista lava dome may have been provoked by eruptive activity that involved dome growth and over steepening, leading to instability. The contribution of strong regional seismic activity could also have played a triggering role, since there is an active, shallow seismic source 30 km to the south which typically generates 6.5–7.0 M_w magnitude shallow (<15 km depth) earthquakes every couple hundred years (Beauval et al., 2013). This seismic activity has offset LGM moraines in the earthquake source area where the main strike-slip fault (Puna-Pallatanga-Cosanga-Chingual) passes through them.

Following the lava dome collapse, more explosive events likely occurred, generating small PDCs and this activity is represented by overcapping co-ignimbritic fine ash layer which has scarce vesicular pumiceous components as well as lithics from the Buenavista dome. However, there is no evidence of thick, massive PDC deposits at any of the studied outcrops.

We attribute the two lithic-rich/tephra layers (A and B) to eruptions that occurred after the collapse event and whose mineralogy corresponds to that of the breccia deposit in the hummocks. These tephra/lithic layers are younger than 44 ky BP, based on our stratigraphic investigations and radiometric dating and indicate rejuvenation of Buenavista dome. As such they represent the latest eruptive activity recognized at Chalupas Caldera involving magma from the Chalupas system. This is an important result, because dates of younger eruptive activity at Chalupas did not exist until now. The deposit of the Buenavista collapse event is not dated, but we hypothesize that it occurred before deposition of the tephra layers A and B. This assertion is

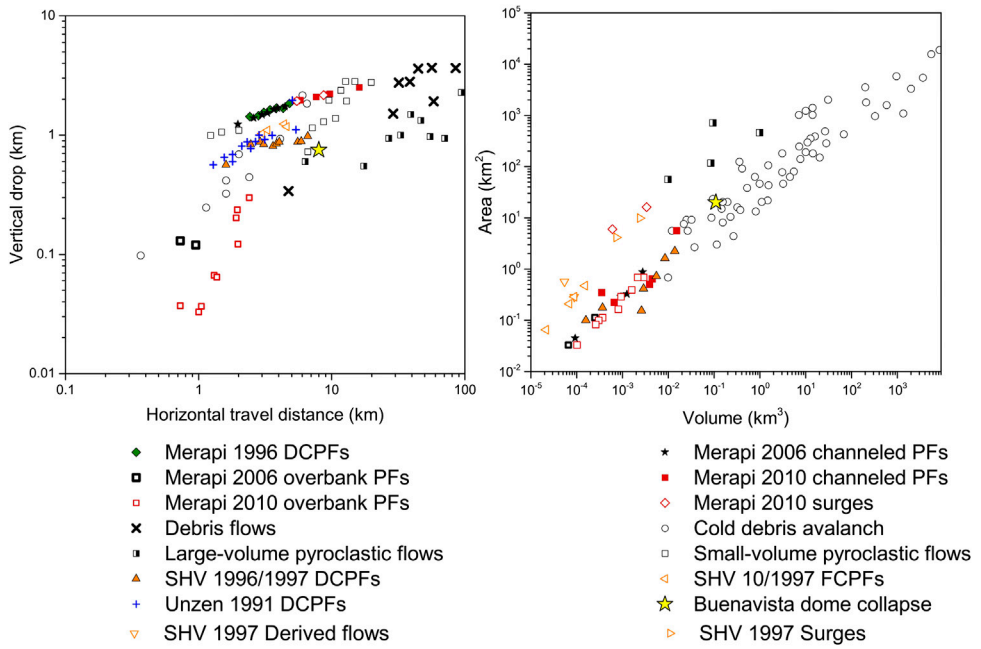

FIGURE 14 | Comparison between various types of flows of dome collapse origin (DCPFs), PFs, debris flows, and cold debris avalanche deposits (from Merapi volcano, Unzen volcano, Soufriere Hills volcano (SHV) and others) with regard to vertical drop over horizontal distance traveled (H/L), and Area (km^2) vs Volume (km^3). Buenavista data are represented with a yellow star, and are located within spaces represented by dome collapse block and ash flows, small-volume pyroclastic flows and cold debris avalanches. Modified from Charbonnier et al. (2013).

based on the presence of the dated tephra layer, CHL-MC-29 (43,620 ± 710 years BP) shown in **Figure 9**, photo B. Immediately beneath the dated tephra is a 5-m-thick fine–grained lithic ash and lacustrine sequence, which is indicative of fine materials being deposited in the local drainage for some time (months to years) in order to accumulate the fine ash lacustrine layers. We hypothesize that the fine lithic ashfall layers that also comprise the section are products of Buenavista lava dome activity. While interbedded layers of pumicious and obsidian shard-rich ash are likely a product of Cotopaxi eruptions.

The vertical drop (km) (H) (0.750 km) from the surmised highest point of the Buenavista collapse initiation to the horizontal distance that the flow traveled (L) (7,000 m) yields an H/L = 0.017. Block and ash flows from dome collapse at Soufriere Hills volcano had an H/L = 0.22 (Voight et al., 2002) and Unzen volcano is associated with H/L = 0.10 (Yamamoto et al., 1993). See also, Ogburn, (2012), for a comprehensive listing of mass flow data and earlier work by Hayashi and Self, (1992). By comparing deposit area to volume (using the 20 km^2 area of the mapped hummock field and the 120 Mm^3 volume derived from the *LaharZ/PFz* modeling), our Buenavista data fall in the category of a cold debris avalanche and also bear similarity to a block-and-ash flow from a lava dome collapse (**Figure 14**, see also Charbonnier et al., 2013). Nevertheless, it is noted that the volume estimate remains uncertain, as the basal topography over which the flow propagated is unknown. The estimate corresponds with simulations that mantle 90% of the hummock area but it can be considered a minimum value, since deposit thickness is highly variable. As observed by Carrasco-Nuñez (1999), the main driving force to obtain far-reaching emplacement of block-and-ash deposits at Citlaltépetl volcano (eastern Mexico) was gravitational collapse and not strong explosivity. We envision a similar situation for Buenavista, where a growing dome became progressively unstable on its eastern limb, and gravitational collapse may have happened successively, perhaps accompanied by some explosivity, but not enough to produce abundant vesicle-rich pyroclastic flows. Perhaps the hummocky nature of the resultant topography on the east Chalupas plain witnesses the contribution of a combination of components of a cold-avalanche and block-and-ash breccias, then later undergoing stream erosion.

Modeling the Buenavista collapse event helped us to appreciate the possible routes that the breccia flows may have taken to deposit the hummocks on the eastern plain and to envision where they might propagate in the future, should Buenavista dome reactivate. Essentially, evidence suggests that the flow propagated east to southeast, where it now outcrops, as our geological field investigations have found. Comparing simulations showed that the rheological parameter, represented by the yield strength values plugged into VolcFlow, can be an important input when trying to simulate the dispersion of dome collapse deposits. The VolcFlow results showed the mass flow heading down three drainages, more than what we can account for in our field mapping. Also this modeling did not show a good replication of the hummock field in the area of highest concentration of hummocks. This shortcoming could be the outcome of not applying an appropriate value for the cohesivity (constant retarding stress) variable

Results of running the *LaharZ/PFz* program covered the majority (~90%) of the area now occupied by the mapped hummock field on the eastern Chalupas plain, satisfactorily representing the final emplacement of the breccia flow on the present-day topography. We believe this is so, because the approximately 20 km^2 depositional area of the hummocks has basically remained the same, i.e., within the confines of the eastern Chalupas plain located between the massif of the dome and the high-relief structures to the east. What has undoubtedly changed is the basal topography over which the flow propagated and where it deposited its material. Using the limits of mapped hummocks is a constraint to help determine a reasonable volume for the deposit, which is the main unknown variable, since in this present study the area occupied by the hummock field has likely not changed significantly in the last 40 ky.

The starting volume of hummocks (10×10^6 m^3) that we initially estimated from the high-resolution DEM is an extreme lower limit. This first exercise led us to assume that the initial volume of hummocks was probably much greater, and that deposit modification was probably due to post-emplacement erosion, compaction, and the impossibility of incorporating all of the buried hummock portion concealed under the Chalupas plain. The modeled scenario that provided the closest approximation to replicating the deposit's footprint employed a volume of 12×10^7 m^3, and its inundation closely mantles (~90%) the mapped hummock area within the confines of the east Chalupas plain.

The remoteness of the eastern portion of the Chalupas caldera would greatly shield the local population in the Inter-Andean Valley (IAV) from strong impacts of gravitational flows should future dome collapse occur within the caldera. Tephra falls from VEI 3 to 5 eruptions would however cause impacts to buildings, public infrastructure and agricultural activities in the IAV, particularly since preferential wind direction generally directs tephra falls to this populated valley.

If there is renewed activity which could potentially include new dome growth in the future and collapse occurs, the route of the Buenavista stream takes it into the Chalupas river. This river is a principal tributary to the Jatunyacu-Napo rivers, located some 60 km downriver on the Amazonian plain. Aggradation by lithic deposits and probable secondary lahars would seriously affect many small villages built along river margins and road transport networks to these areas, located to the S and E of the provincial capital of Tena, in Napo Province. These areas have already been inundated by primary lahars born on Cotopaxi volcano (Sierra et al., 2019).

CONCLUSION

Our field mapping of hummocky terrain, sampling and radiometric dating of associated tephra layers in stream cuts, and analysis of SEM images suggest that the probable origin of hummocky terrain on the eastern plain of Chalpas caldera is a gravitational mass flow sourced from the Buenavista Dome. Stratigraphic constraints on the deposit provide a relative age for the most recent activity at Buenavista Dome, giving us insight into the youthfulness of the late stages of Chalupas activity.

Our study has shown that the last eruptive activity at Chalupas Caldera occurred about 40 ka ago and is represented by several post-collapse tephra layers, especially those named "A" and "B." Based on geochemistry, lithic componentry and the mineralogical suite of the tephra falls, the source vent likely belongs to the Buenavista dome complex. Antecedent to emission of the tephra falls was a collapse of the eastern flank of Buenavista lava dome complex. The collapse of the dome is represented by hummocky topography traceable from the eastern toe of Buenavista dome and spreading eastward upon a topographically-confined plain over a 20 km^2 area and extending southward at least 7 km. The area is basically hemmed in by older non-volcanic ridges and the parent dome. A minimal, order-of-magnitude estimate of the volume of the hummock field (120 Mm^3) is supported by numerical modeling using the present-day topography and achieving a reasonable overlay between modeling with the program *LaharZ/PFz* and the mapped limits of the hummock field on present-day topography. We believe that the basal topography has changed in the last 40 ka, but that the depositional area has experienced fewer changes.

The rocks and matrix collected from hummocks show strong similarities to samples taken from Buenavista dome. Given this similarity, the position of the hummock field at the base of the unbuttressed eastern flank of Buenavista, and visual recognition of a scar on the eastern shoulder of this dome, we believe that the most likely origin of the hummock field is a gravitational slide off of the Buenavista Dome Complex.

Comparison of the Buenavista H/L ratio and inundated area vs volume with cohorts of other volcanoes places the Buenavista breccia deposits in the categories of cold avalanche deposits and block-and-ash lava dome collapse breccia deposits (**Figure 14**). Therefore, we conclude that the provenance of the hummock field on the eastern Chalupas plain is a product of a gravitational slide off the eastern limb of Buenavista dome that occurred before 44 ky BP.

If a collapse occurred at Buenavista dome today with a volume of ~120 million m^3 or greater it would expand both eastward and southward to likely occupy the footprint left by the Buenavista event of ~40 ky. Breccia flows would also divulge into the Huahui and Chalupas rivers, and transform to secondary lahars over the 60 km distance to the Amazonian lowlands. Riverside-dwelling populations along the distal Napo river would be affected. At the moment, no geophysical indications (seismic or deformation) of unrest are detected by the instrumental monitoring carried out by the Instituto Geofísico of the Escuela Politécnica Nacional in Quito.

The modeling exercise as presented here is probably best considered as a reconnaissance-like first evaluation of potential breccia volumes to be modeled for future Buenavista dome collapse and assess which river channels would most likely be inundated by gravitational mass flows and subsequently, their possible transformation downstream to secondary lahars. On a broader scale, following lava dome collapse and regrowth cycles, river channels are often overloaded with lithic debris and the displaced water will occupy wider inundation zones, flooding the bottomlands. The aggradation of the lithic material may also infill channels and bury bridges and river-side infrastructure. These morphological changes may also occur far downstream as a result of lava dome activity, especially if it is long-lasting and voluminous.

DATA AVAILABILITY STATEMENT

The raw data supporting the conclusions of this article will be made available by the authors, without undue reservation, to any qualified researcher.

AUTHOR CONTRIBUTIONS

MC: Analysis of DEM and orthophotos, fieldwork, drone survey, computational simulations, investigation, petrography, geochemistry interpretation, writing—original draft, review and editing. PM: Investigation, conceptualization, fieldwork, stratigraphy, resources, writing—review and editing, supervision. JS: Analysis of DEM and orthophotos, fieldwork, drone survey, investigation, resources, writing—review and editing. HG: Investigation, fieldwork, drone survey, SEM analysis, resources, writing—review and editing.

FUNDING

The first phase of this project was funded by the Instituto Geofísico de la Escuela Politécnica Nacional through the project "SENPLADES- Generación de Capacidades para la Emisión de Alertas Tempranas" covering travel and logistics during fieldwork. In early 2019, the Escuela Politécnica Nacional awarded us the research project "Proyecto Semilla PIS-18-02" whose title is: *Geologic and petrological study of the eruptive products of the Chalupas Caldera*, which covered fieldwork expenses, some radiometric dates and publication costs. We kindly thank both institutions for providing financial and administrative support for this project.

ACKNOWLEDGMENTS

We thank the Instituto Geofísico of the Escuela Politécnica Nacional (IG-EPN) in Quito for logistical support and help with other intangibles. We kindly thank Lisa Hammersley for permitting us to use her extensive geochemical database from her doctoral dissertation at the University of California, Berkeley. We thank Ings. Bernardo Beate and Pedro Espin for kindly reviewing a draft of this manuscript. We would like to thank to Karim Kelfoun for providing the license of the numerical code VolcFlow, developed at the Laboratoire Magmas et Volcans, Clermont Ferrand, used for making the numerical simulations. We thank Silvia Vallejo for her help in VolcFlow modeling. And we thank USGS for their Lahar_Z open access software available on their web page. We would like to thank the project "Strengthening Resilience in Volcanic Areas" (STREVA), funded by the Natural Environment Research Council (NERC) and the Economic and Social Research Council (ESRC), (Great Britain), who provided the drone model eBee classic used to conduct this research. We thank Jorge Aguilar from the Instituto Geofísico de la Escuela Politécnica Nacional, for his continuous support in calculating the hummock volumes using his proposed script. We also thank the staff of DEMEX-EPN, particularly Ing. Evelyn Criollo, for assistance with the SEM analysis of the rock samples. The authors also especially thank Ing. Fernando Cobo, owner of Hacienda Yanahurco, and the local Chagras (Andean cowboys), for their enthusiastic help during the long days of fieldwork and horseback excursions in this beautiful caldera. Thanks to Jorge J. Anhalzer for his willingness to provide excellent photos and flying time in the caldera. Thanks to Jennifer Garrison and Ken Sims for assistance with sample processing, shared discussions and idea enrichment! Thanks to our two reviewers, and the editor Pablo Tierz, all who gave careful and demanding revisions that substantially improved our manuscript.

REFERENCES

Aguilar, J. (2013). *Cálculo del volumen de un volcán.* Quito, Ecuador: Instituto Geofísico de la Escuela Politécnica Nacional, 7.

Bablon, M., Quidelleur, X., Siani, G., Samaniego, P., Le Pennec, J.-L., Nouet, J., et al. (2020). Glass shard K-Ar dating of the Chalupas caldera major eruption: main Pleistocene stratigraphic marker of the Ecuadorian volcanic arc. *Quat. Geochronol.* 57, 101053. doi:10.1016/j.quageo.2020.101053

Baby, P., Rivadeneira, M., Barragán, R., and Christophoul, F. (2013). Thick-skinned tectonics in the oriente foreland basin of Ecuador. *Geolo. Soci., London, Spec. Publ.* 377, 59–76. doi:10.1144/SP377.1

Bachmann, O., and Bergantz, G. (2008). The magma reservoirs that feed supereruptions. *Elements.* 4, 17–21. doi:10.2113/GSELEMENTS.4.1.17

Beate, B. (1985). "El flujo piroclástico de Chalupas como causante de un desastre natural en el Cuaternario de los Andes Septentrionales del Ecuador," in *Primer simposio latinoamericano sobre desastres naturales.* Quito, Ecuador, 21–27.

Beate, B. (1989). IAVCEI – sta. Fe, New Mexico. abstract: the Chalupas ignimbrite. *N. M. Bur. Mines Mine. Resour. Bull.* 131, 18.

Beate, B., Hammersley, L., DePaolo, D., and Deino, A. (2006). La edad de la ignimbrita de Chalupas, Prov. de Cotopaxi, Ecuador, y su importancia como marcador estratigráfico. *Resúmenes Sex. J. Cienc. Tierra.* 1, 68–71.

Beauval, C., Yepes, H., Palacios, P., Segovia, M., Alvarado, A., Font, Y., et al. (20132013). An earthquake catalog for seismic hazard assessment in Ecuador. *Bull. Seismol. Soc. Am.* 103, 773–786. doi:10.1785/0120120270

Cardona, C., Pulgarín, B., Agudelo, A., Calvache, M., Ordoñez, M., and Manzo, O. (2015). Ajuste del método lahar-Z en el sector del volcán Nevado del Huila, con base en los flujos de escombros de 1994 y 2007. *Bol. Geol. Colomb.* 43, 63–74. doi:10.32685/0120-1425/boletingeo.43.2015.30

Carrasco-Núñez, G. (1999). Holocene block-and-ash flows from summit dome activity of Citlaltépetl volcano, Eastern Mexico. *J. Volcanol. Geoth. Res.* 88, 47–66. doi:10.1016/S0377-0273(98)00110-3

Charbonnier, S. J., Germa, A., Connor, C. B., Gertisser, R., Preece, K., Komorowski, J.-C., et al. (2013). Evaluation of the impact of the 2010 pyroclastic density currents at Merapi volcano from high-resolution satellite imagery, field investigations and numerical simulations. *J. Volcanol. Geoth. Res.* 261, 295–315. doi:10.1016/j.jvolgeores.2012.12.021

Clapperton, C. M. (1993). *Quaternary geology and geomorphology of South America.* Amsterdam, The Netherlands: Elsevier, 779.

Clapperton, C. M., Hall, M., Mothes, P., Hole, M. J., Still, J. W., Helmens, K. F., et al. (1997). A younger Dryas icecap in the equatorial Andes. *Quat. Res.* 47, 13–28. doi:10.1006/qres.1996.1861

Córdova, M. D. (2018). Identificación y caracterización de los últimos productos eruptivos de a fase resurgente de la Caldera de Chalupas. Quito, Ecuador: Escuela Politécnica Nacional, Vol. 133. Available at: http://bibdigital.epn.edu.ec/handle/15000/19286.

Córdova, M. D., Mothes, P. A., Hall, M. L., and Telenchana, E. (2018). "Identification and characterization of the youngest eruptive products of the Chalupas Caldera, Ecuador: an update on the caldera," in Abstract volume of the international meeting Cities on Volcanoes, 10, Naples, Italie, 682.

Crandell, D. R., Miller, C. D., Glicken, H. X., Christiansen, R. L., and Newhall, C. G. (1984). Catastrophic debris avalanche from ancestral Mount Shasta volcano, California. *Geology.* 12, 143–146. doi:10.1130/0091-7613(1984)12<143:CDAFAM>2.0.CO;2

De Angelis, S. H., Larsen, J., Coombs, M., Dunn, A., and Hayden, L. (2015). Amphibole reaction rims as a record of pre-eruptive magmatic heating: an experimental approach. *Earth Planet Sci. Lett.* 426, 235–245. doi:10.1016/j.epsl.2015.06.051

Encalada, M., and Bernard, B. (2018). "Dynamics of Cotopaxi volcano debris avalanche," in Abstract volume of the international meeting cities on volcanoes, 10, Naples, Italie, 682.

Fiorini, E., and Tibaldi, A. (2011). Quaternary tectonics in the central Interandean Valley, Ecuador: fault-propagation folds, transfer faults and the Cotopaxi Volcano. *Global Planet. Change.* 90–91, 87–103. doi:10.1016/j.gloplacha.2011.06.002

Fruendt, A., Wilson, C. F. N., and Carey, S. N. (2000). "Ignimbrites and block and ash flow deposits," in *Encyclopedia of volcanoes.* Editor H. Sigurdesson (San Diego, CA: Academic Press), 581–600.

Garrison, J. M., Davidson, J. P., Hall, M., and Mothes, P. (2011). Geochemistry and petrology of the most recent deposits from Cotopaxi volcano, NorthernVolcanic Zone, Ecuador. *J. Petrol.* 52, 1–38. doi:10.1093/petrology/egr023

Glicken, H. (1996). U.S. Geological Survey Open-File Report 96-677. Rockslide-debris Avalanche of May 18, 1980. Washington, DC: Mount St. Helens 983 Volcano, 90. Available at: https://pubs.usgs.gov/of/1996/0677/ (Accessed December 4, 2020).

Guillier, B., Chatelain, J. L., Jaillard, E., Yepes, H., Poupinet, G., and Fels, J. F. (2001). Seismological evidence on the geometry of the orogenic system in central-northern Ecuador (South America). *Geophys. Res. Lett.* 28 (19), 3749–3752. doi:10.1029/2001GL013257

Hall, M., and Mothes, P. (2008). The rhyolitic–andesitic eruptive history of Cotopaxi volcano, Ecuador. *Bull. Volcanol.* 70, 675–702. doi:10.1007/s00445-007-0161-2

Hall, M. L., Samaniego, P., Le Pennec, J.-L., and Johnson, J. B. (2008). Ecuadorian Andes volcanism: a review of Late Pliocene to present activity. *J. Volcanol. Geoth. Res.* 176, 1–6. doi:10.1016/j.jvolgeores.2008.06.012

Hammersley, L. C. (2003). Isotopic evidence for the relative roles of fractional crystallization, crustal assimilation and magma supply in the generation of large volume rhyolitic eruptions. Ph.D. Dissertation. Berkeley, (CA): University of California.

Hammersley, L., and De Paolo, D. J. (2002). "Oxygen isotope evidence for the role of crustal contamination in the evolution of the Chalupas caldera system, northern Andes, Ecuador," in AGU fall meeting, San Francisco, CA, December [abstract].

Hastenrath, S. (1981). *The glaciation of the Ecuadorian Andes.* Rotterdam, Balkema, 159.

Hayashi, J. N., and Self, S. (1992). A comparison of pyroclastic flow and debris avalanche mobility. *JGR: Solid Earth.* 97 (B6), 9063–109071. doi:10.1029/92JB00173

Heine, K., (2004). Late quaternary glaciations of Ecuador. *Dev. Quat. Sci.* 2, 165–169. doi:10.1016/S1571-0866(04)80121-0

Hidalgo, S., Gerbe, M. C., Martin, H., Samaniego, P., and Bourdon, E. (2012). Role of crustal and slab components in the northern Volcanic zone of the Andes (Ecuador) constrained by Sr–Nd–O isotopes. *Lithos.* 132 (133), 180–192. doi:10.1016/j.lithos.2011.11.019

INECEL (1983). Estudio de exploración de los recursos geotérmicos en Chalupas, Primera fase de prefactibilidad. Unpublished Technical Report, Quito Ecuador.

Iverson, R. M., Schilling, S. P., and Vallance, J. W. (1998). Objective delineation of lahar-inundation hazard zones. *GSA Bull.* 110, 972–984. doi:10.1130/0016-7606(1998)110<0972:ODOLIH>2.3.CO;2

Jackson, L. J., Horton, B. K., Beate, B. O., Bright, J., and Breecker, D. O., (2019). Testing stable isotope paleoaltimetry with quaternary volcanic glasses from the Ecuadorian Andes. *Geology.* 47, 1–4. doi:10.1130/G45861.1

Kelfoun, K., and Druitt, T. H. (2005). Numerical modeling of the emplacement of socompa rock avalanche, Chile. *J. Geophys. Res.* 110, B12202. doi:10.1029/2005JB003758

Kelfoun, K., Samaniego, P., Palacios, P., and Barba, D. (2009). Testing the suitability of frictional behaviour for pyroclastic flow simulation by comparison with a well-constrained eruption at Tungurahua volcano (Ecuador). *Bull. Volcanol.* 71, 1057–1075. doi:10.1007/s00445-009-0286-6

Lipman, P. W. (1997). Subsidence of ash-flow calderas: relation to caldera size and magma-chamber geometry. *Bull. Volcanol.* 59 (1997), 198–218.

Marrero, J. M., Vasconez, F., Espín, P., Ortiz, R., Yepes, H., García, A., et al. (2019). MDTanaliza: understanding digital elevation models when facing gravity-driven flows in a hazard assessment context. *Earth Sci. Inform.* 12, 257–274. doi:10.1007/s12145-018-0372-4

Mothes, P. A., Hall, M. L., and Janda, R. (1998). The enormous Chillos Valley Lahar: an ash-flow-generated debris flow from Cotopaxi volcano, Ecuador. *Bull. Volcanol.* 59, 233–244.

Mothes, P. A., and Hall, M. L. (2008). "Rhyolitic calderas and centers clustered within the active andesitic belt of Ecuador's eastern Cordillera," in IOP conference series: earth and environmental science. IOP Publishing, 012007.E Available at: https://iopscience.iop.org/article/10.1088/1755-1307/3/1/012007.

Nocquet, J., Villegas-Lanza, J., Chlieh, M., Mothes, P. A., Rolandone, F., Jarrin, P., et al. (2014). Motion of continental slivers and creeping subduction in the northern Andes. *Nat. Geosci.* 7, 287–291. doi:10.1038/ngeo2099

Ogburn, S. E. (2012). FlowDat: mass flow database v2.2. On Vhub. Available at: https://vhub.org/groups/massflowdatabase (Accessed December 4, 2020).

Ordoñez, J., Vallejo, S., Bustillos, J., Hall, M., Andrade, D., Hidalgo, S., et al. (2011). *Volcan Sangay, Mapa de Peligros Volcánicos Potenciales. 1:50,000.* Quito, Ecuador: Instituto Geofisico, Escuela Politécnica Nacional. Available at: https://www.igepn.edu.ec/sangay-mapa-de-peligros.

Özdemir, Y., Akkaya, İ., Oyan, V., and Kelfoun, K. (2016). A debris avalanche at Süphan stratovolcano (Turkey) and implications for hazard evaluation. *Bull. Volcanol.* 78 (2), 1–13.

Paguican, E. M. R., van Wyk de Vries, I. B., and Lagmay, I. A., (2012). Hummocks: how they form and how they evolve in rockslide-debris avalanches. *Landslides.* 11, 67–80. doi:10.1007/s10346-012-0368-y

Pérez, G. (2020). *Caracterización de las fisuras eruptivas y morfologías de los volcanes Wolf y Alcedo del Archipiélago de Galápagos: aporte a la evaluación de amenaza volcánica.* Quito, Ecuador: Escuela Politécnica Nacional. Available at: https://bibdigital.epn.edu.ec/handle/15000/20686.

Robin, C., Samaniego, P., Le Pennec, J.-L., Fornari, M., Mothes, P., and van der Plicht, J. (2010). New radiometric and petrological constraints on the evolution of the Pichincha volcanic complex (Ecuador). *Bull. Volcanol.* 72, 1109–1129. doi:10.1007/s00445-010-0389-0

Schilling, S. P. (2014). Laharz_py: GIS tools for automated mapping of lahar inundation hazard zones. US Department of the Interior, Geological Survey doi:10.3133/ofr20141073

Sierra, D., Vasconez, F., Andrade, D., Almeida, M., and Mothes, P. (2019). Historical distal lahar deposits on the remote eastern-drainage of Cotopaxi volcano, Ecuador. *J. S. Am. Earth Sci.* 95, 102251. doi:10.1016/j.jsames.2019.102251

Sparks, R. S. J., Barclay, J., Calder, E. S., Herd, R. A., Komorowski, J. C., Luckett, R. G., et al. (2002). "Generation of a debris avalanche and violent pyroclastic density current on 26 December (Boxing Day) 1997 at Soufriere Hills Volcano, Montserrat," *The eruption of Soufriere Hills volcano, Montserrat, from 1995 to 1999. Geological society, London, memoirs, 21.* (London, England: Editors T. H. Druitt and b. P. KokelaarThe Geological Society of London), 409-434. 0435-4052/02/S15 r.

Spikings, R. A., Cochrane, R., Villagomez, D., Van Der Lelij, R., Vallejo, C., Winkler, W., et al. (2015). The geological history of northwestern South America: from Pangaea to the early collision of the Caribbean large igneous province (290–75Ma). *Gondwana Res.* 27 (1), 95–139. doi:10.1016/j.gr.2014.06.004

Spikings, R. A., Winkler, W., Seward, D., and Handler, R. (2001). Along-strike variations in the thermal and tectonic response of the continental Ecuadorian Andes to the collision with heterogeneous oceanic crust. *Earth Planet Sci. Lett.* 186, 57–73. doi:10.1016/S0012-821X(01)00225-4

Stoopes, G. R., and Sheridan, M. F. (1992). Giant debris avalanches from the Colima Volcanic Complex, Mexico, Implication for long runout landslides (>100 km). *Geology.* 20, 299–302. doi:10.1130/0091-7613(1992)020<0299:GDAFTC>2.3.CO;2

Tost, M., Cronin, S. J., and Procter, J. N. (2014). Transport and emplacement mechanisms of channelized long-runout debris avalanches, Ruapehu volcano, New Zealand. *Bull. Volcanol.* 76 (12), 1–14.

Ui, T., Takarada, S., and Yosimoto, M. (2000). "Debris avalanches,"in *Encyclopedia of volcanoes.* Editor H. Sigurdsson (San Diego, CA: Academic Press), 617–626.

Vásconez, F. J., Andrade, D., and Valverde, V. (2015). The deposits of Pululahua Volcanic Complex (PVC), Ecuador: estimation of the erupted magma mass/volume. Prague, The Czech Republic. Available at: https://www.researchgate.net/publication/289994184_The_deposits_of_Pululahua_Volcanic_Complex_PVC_Ecuador_estimation_of_the_erupted_magma_massvolume (Accessed December 4, 2020).

Vallejo, C., Spikings, R. A., Horton, B. K., Luzieux, L., Romero, C., Winkler, W., et al. (2019). Late Cretaceous to Miocene stratigraphy and provenance of the coastal forearc and Western Cordillera of Ecuador: evidence for accretion of a single oceanic plateau fragment," in *Andean Tectonics.* Elsevier, 209–236.

van Wyk de Vries, B., and Davies, T. (2015). "Landslides, debris avalanches, and volcanic gravitational deformation," in *Encyclopedia of volcanoes.* Editors H. Sigurdsson, B. Houghton, S. McNutt, H. Rymer, and J. Stix, 2nd Edn. (665–684). Available at: http://dx.doi.org/10.1016/B978-0-12-385938-9.00038-9.

Voight, B., Glicken, H., Janda, R. J., and Douglas, P. M. (1981). "Catastrophic rockslide avalanche of May 18," in *The 1980 eruptions of Mount St. Helens.* Editors P. W. Lipman and D. R. Mullineaux (Washington, DC: US Geological Survey). Professional Paper, 1250, 347–377.

Voight, B., Glicken, H., Janda, R. J., and Douglass, P. M. (1983). Nature and mechanics of the Mount St Helens rockslide-avalanche of 18 May 1980. *Geotechnique.* 33, 243–273.

Voight, B., Komorowski, J.-C., Norton, G., Belousov, A., Belousova, M., Boudon, G., et al. (2002). The 26 december (boxing day) 1997 sector collapse and debris avalanche at Soufriere Hills volcano, Montserrat. London, UK: Geological Society, 21. doi:10.1144/GSL.MEM.2002.021.01.17

White, S. M., Trenkamp, R., and Kellogg, J. N. (2003). Recent crustal deformation and the earthquake cycle along the Ecuador–Colombia subduction zone. *Earth Planet Sci. Lett.* 216, 231–242. doi:10.1016/S0012-821X(03)00535-1

Widiwijayanti, C., Voight, B., Hidayat, D., and Schilling, S. P. (2009). Objective rapid delineation of areas at risk from block-and-ash pyroclastic flows and surges. *Bull. Volcanol.* 71, 687–703. doi:10.1007/s00445-008-0254-6

Yamamoto, T., Takarada, S., and Suto, S. (1993). Pyroclastic flows from the 1991 eruption of Unzen volcano. *Japan. Bull. Volcanol.* 55, 166–175. doi:10.1007/BF00301514

Yepes, H., Audin, L., Alvarado, A., Beauval, C., Aguilar, J., Font, Y., et al. (2016). A new view for the geodynamics of Ecuador: implication in seismogenic source definition and seismic hazard assessment. *Tectonics.* 35 (5), 1249–1279. doi:10.1002/2015TC003941

Conflict of Interest: The authors declare that the research was conducted in the absence of any commercial or financial relationships that could be construed as a potential conflict of interest.